Bridging biological scales by linking agent-based models to intracellular and continuum biomechanics models

Shayn Peirce-Cottler, Ph.D.

Associate Professor of Biomedical Engineering

4.17.13

The DEPARTMENT *of* BIOMEDICAL ENGINEERING

School of Engineering and Applied Science • School of Medicine

Outline

- Introduction to ABM
- Multiscale Modeling
- ABM as a “bridge” in multiscale models
  - Linking ABM to intracellular models
  - Linking ABM to tissue-level biomechanics models
- Summary
- Future Work

Citation

Introduction to ABM

Emergent Phenomena

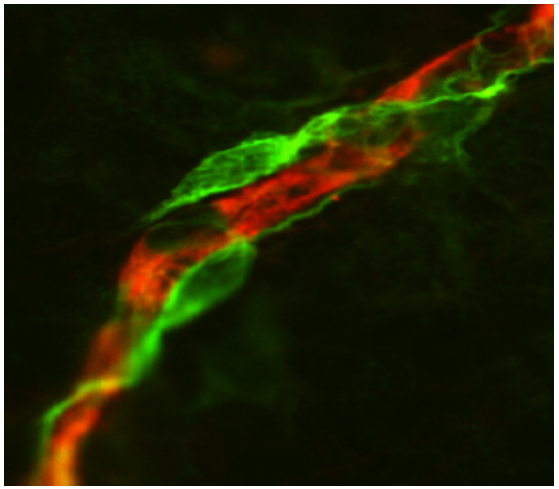

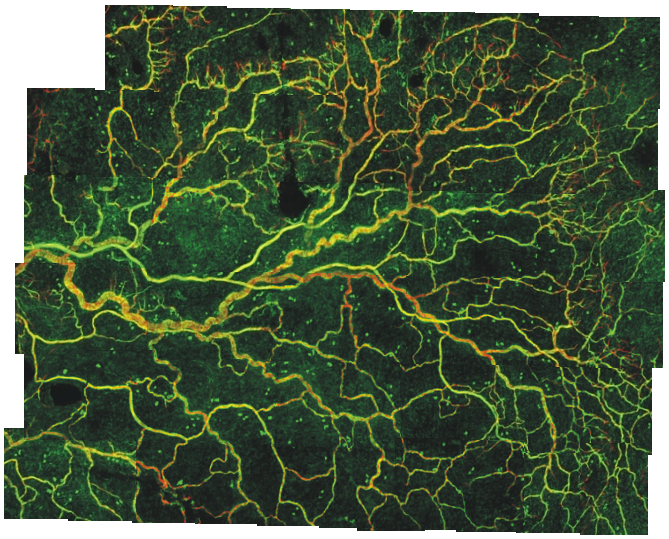

Agent-Based Modeling of Cells

. **Discrete agents represent cells**

. **Agents interact with each other and with their environment**

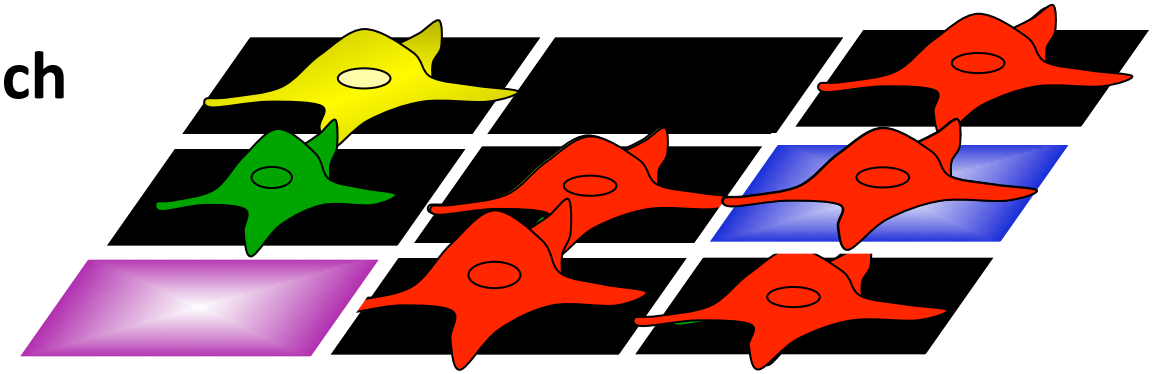

. **Agent behaviors are governed by *(literature-based)* rules**

Agent-Based Modeling of Cells

Netlogo Example

Agent Rules

11: cell behaviors

85: adhesion molecule expression

69: chemokine production & activation

30: integrin activation

~200 total rules

~600+ papers

Agent-based Models

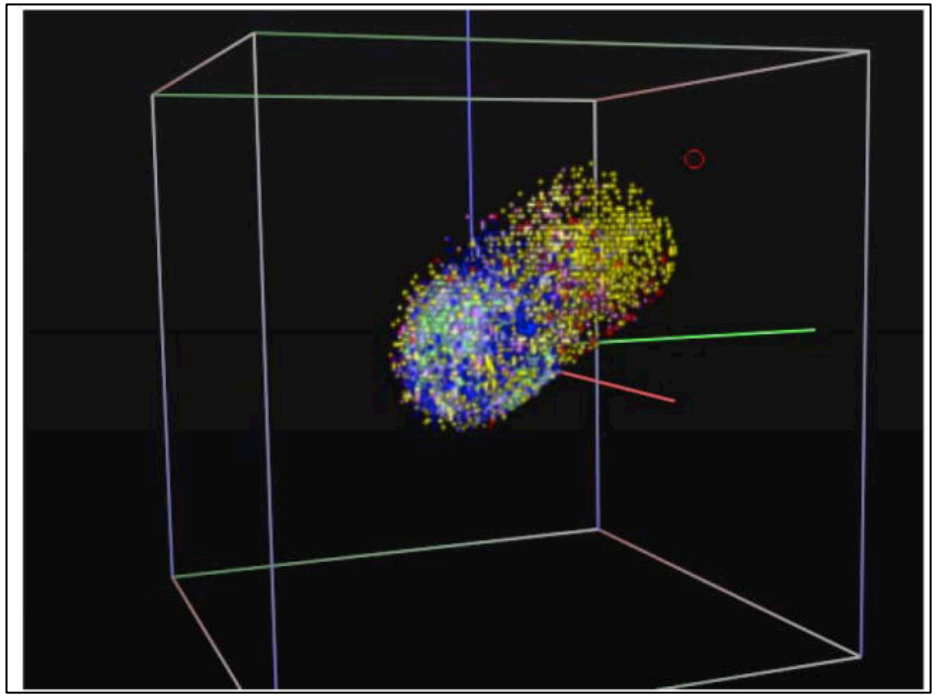

T.S. Deisboeck, 2000

Agent-based Models

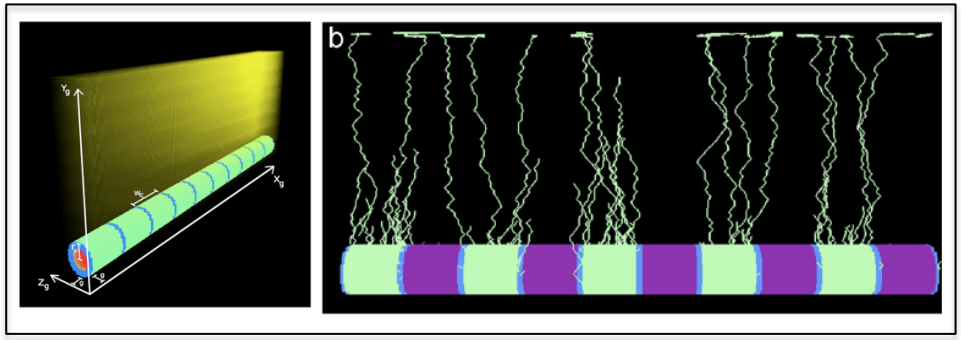

K. Bentley et al. 2008

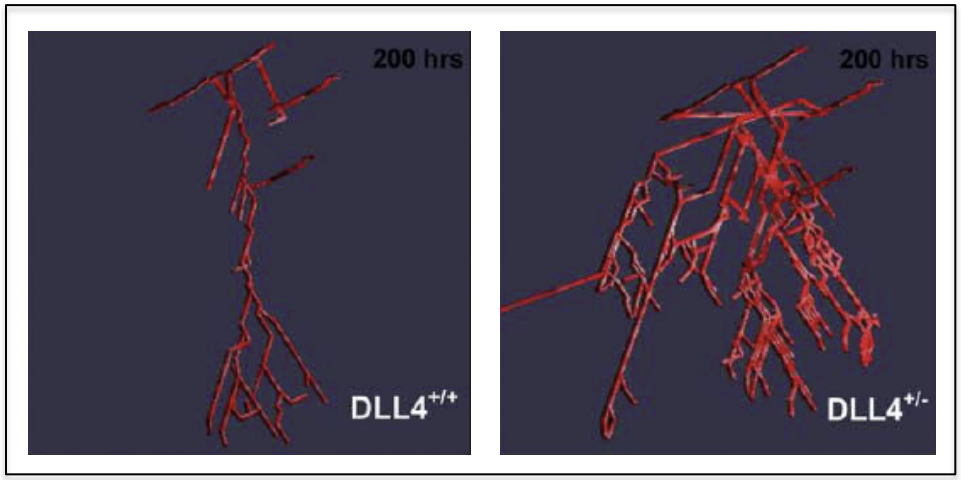

A.Qutub & A. Popel, 2009

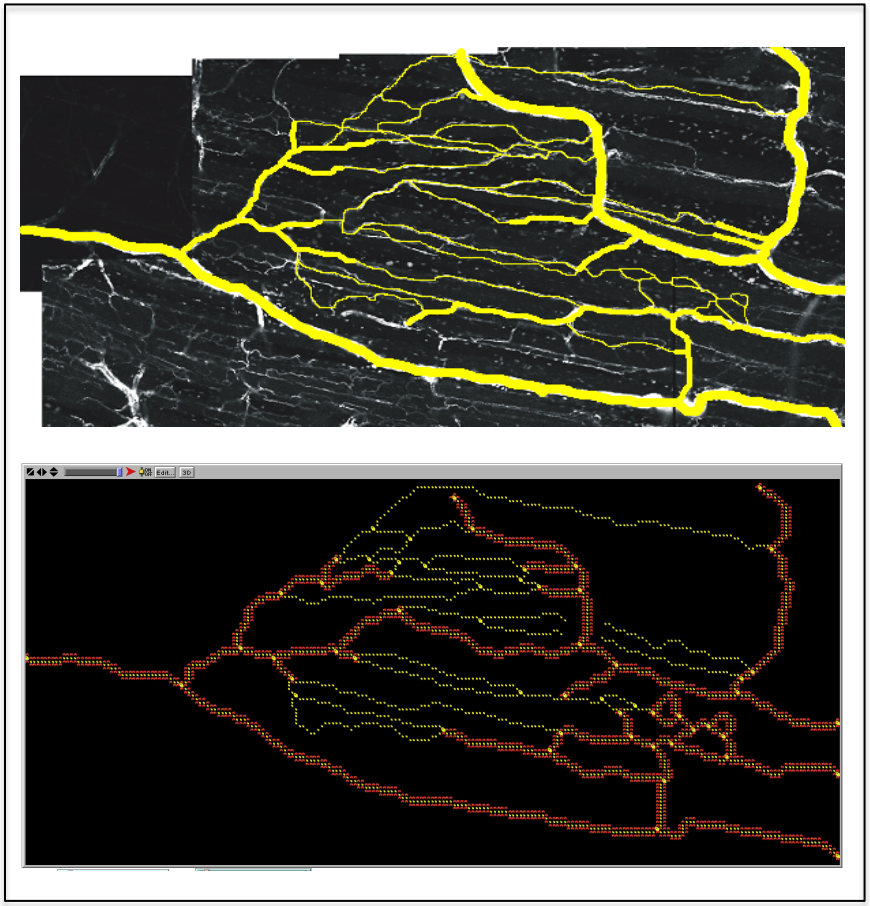

A. Bailey et al. 2009

Agent-based Models

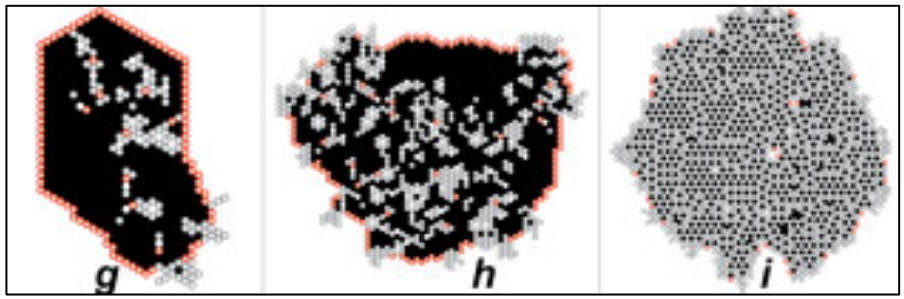

S.H. Kim, J. Debnath, K. Mostov, S. Park, C.A. Hunt (2009)

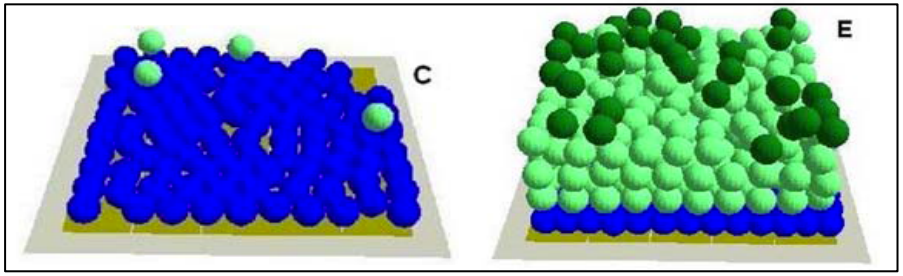

S. Adra , T. Sun, S. MacNeil, M. Holcombe, R. Smallwood (2010)

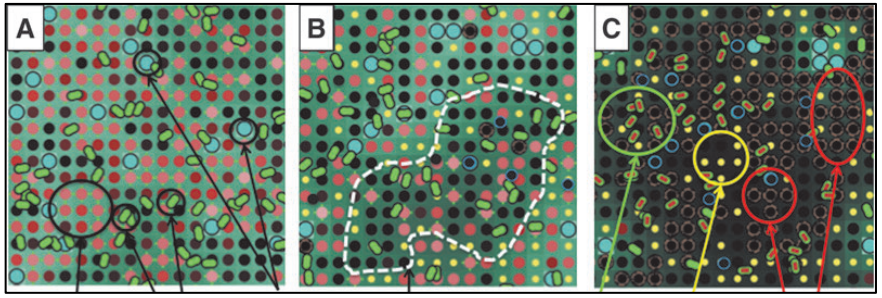

M. Kim, S. Christley, J.C. Alverdy, D. Liu, G. An (2012)

B.N. Brown, I.M. Price, F.R. Toapanta, D. R. DeAlmeida, C.A. Wiley, T.M. Ross, T.D. Oury, Y. Vodovotz (2011)

Multiscale Modeling

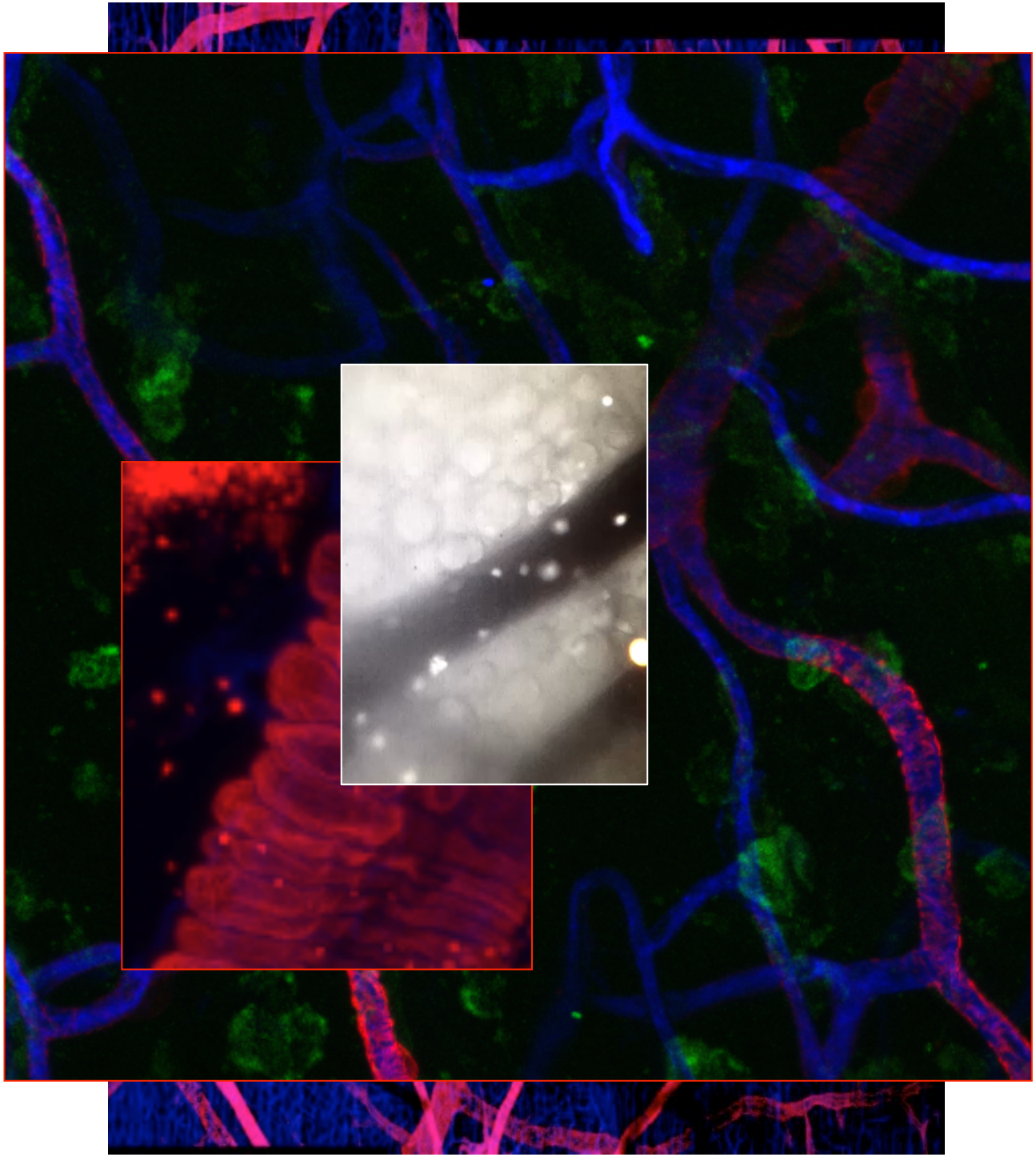

Organism

Organ & Tissue

Multi-Cell

Intracellular

Gene / Protein

…

Time

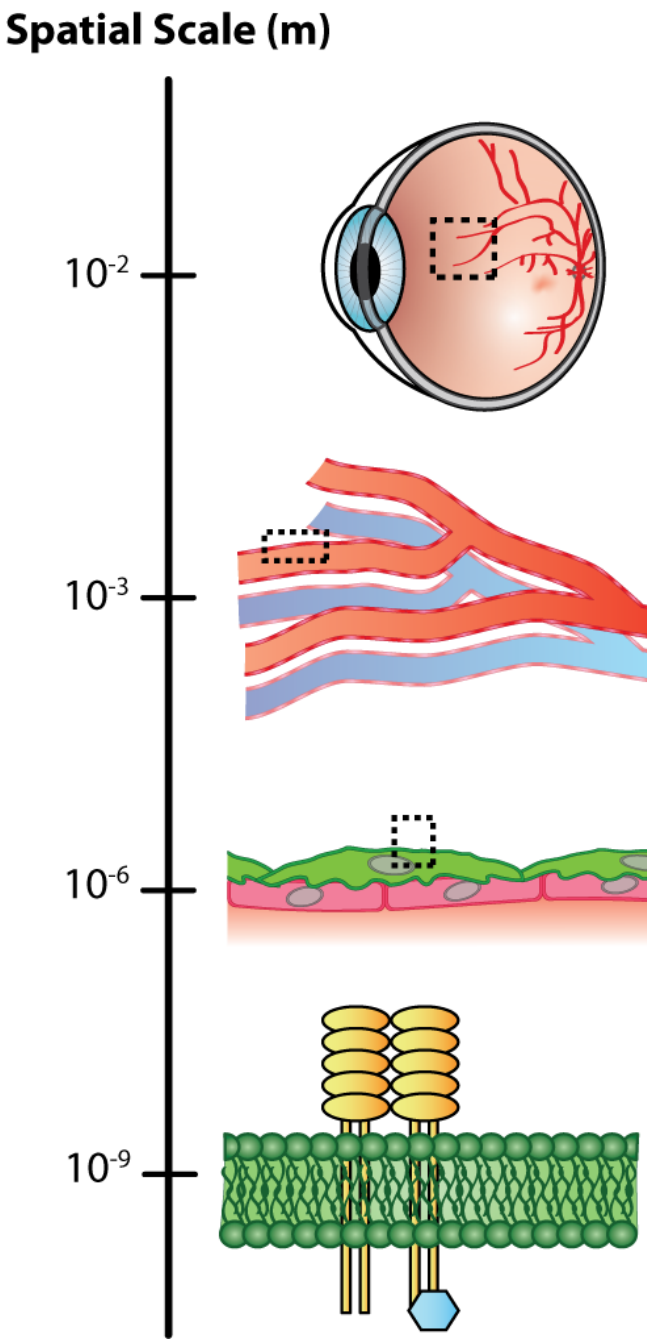

Pathophisiology

At the organ level, **retinal detachment** can occur due to fibrosis of the basement membrane. Though taking only hours to days for complete detachment and **blindness**, this level of damage is end-stage; after years of fibrovascular remodeling, the retina is mechanically evulsed from the underlying tissue.

Tissue level changes of the **microvasculature** reveal **micro-hemorrhages** as a result of vessel wall disruption. In proliferative disease, **neovascularization** is apparent in the periretinal vascular beds. These are the earliest clinical signs and are pathognomonic of the disease. Disregulation of vessel permeability can lead to **macular edema** and vessel dilatation.

Vessel instability can be directly attributed to **apoptotic cell death** of pericytes and **uncoordinated proliferation** of endothelial cells. These changes occur throughout the course of the disease and are relevant both on short- and long-term time resolutions.

Pericyte apoptosis is triggered due to **dephosphorylation** of PDGF receptors, resulting in reduced survival signaling. This disruption is caused by PKC-delta activation and downstream phosphatase activity. These effects can be measured within **days of exposure to hyperglycemia** and are often persistent and irreversible. A simlar mechanism is responsible for endothelial proliferation.

Measurement Techniques

This is a **macroscopic** event that is most easily observed using a standard opthalmascope.

Microscopic flame hemorrhages may be present on opthalmascopic exam. In addition, **cotton-wool spots** are often apparent due to local ischemic injury. Definitive measurements of permeability can be completed with **fundoscopic exam** and **fluorescein angiography**.

Pericyte drop out is typically measured microscopically using **immunihisto-chemical staining** of excised tissues. These observations can be made in murine models of diabetic retinopathy and are commonly studied as indicators of therapeutic efficacy.

Measurements of intracellular signalling are carried out using conventional **molecular biology techniques** such as immunoblotting, in situ hybridization, immunohistochemistry, and immunopre-cipitation. **In vitro** assays and **in vivo** models provide tissue samples for analysis.

J. Walpole, J.A. Papin, S.M. Peirce (in press)

Multiscale Models

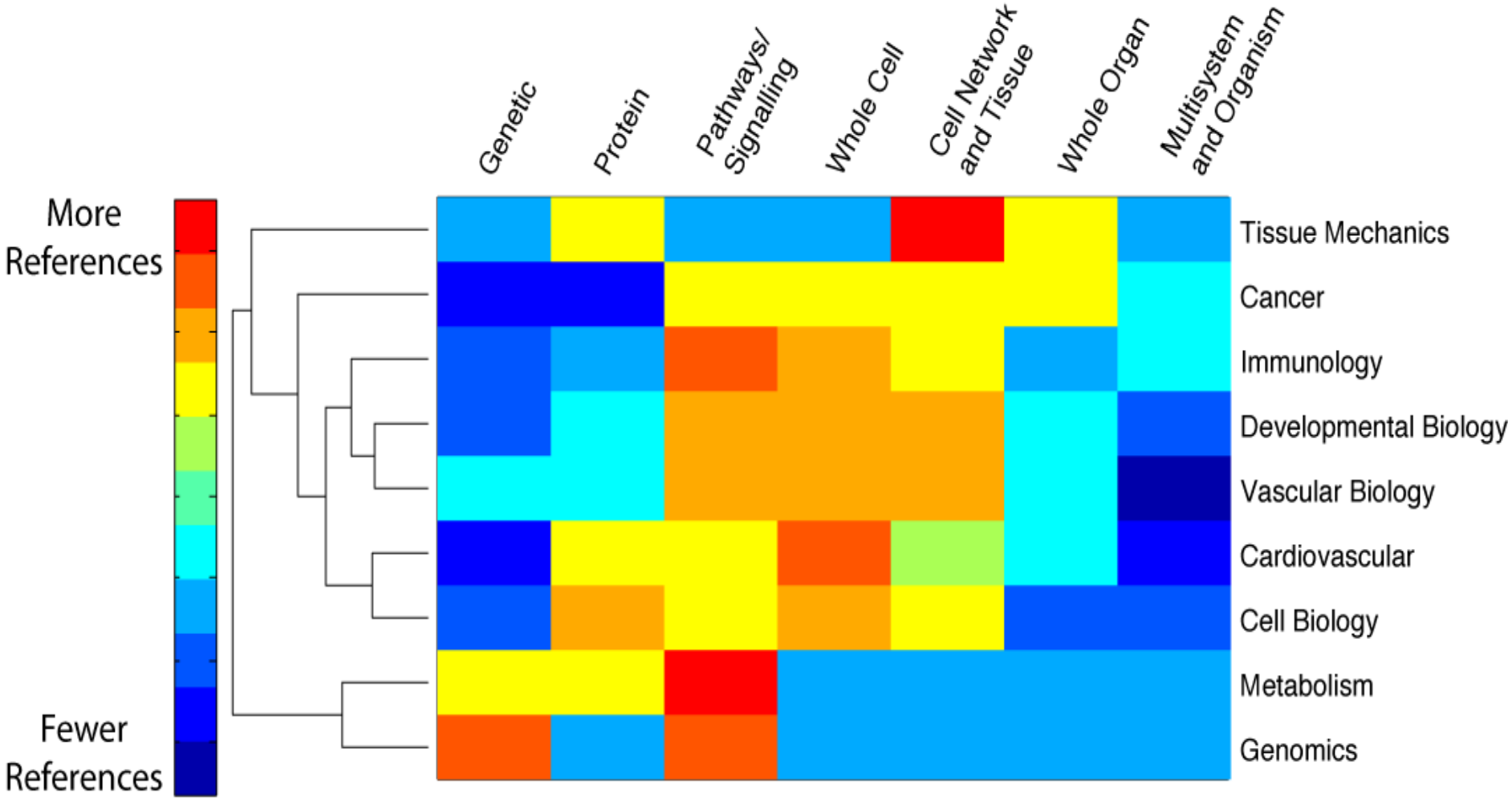

J. Walpole, J.A. Papin, S.M. Peirce (in press)

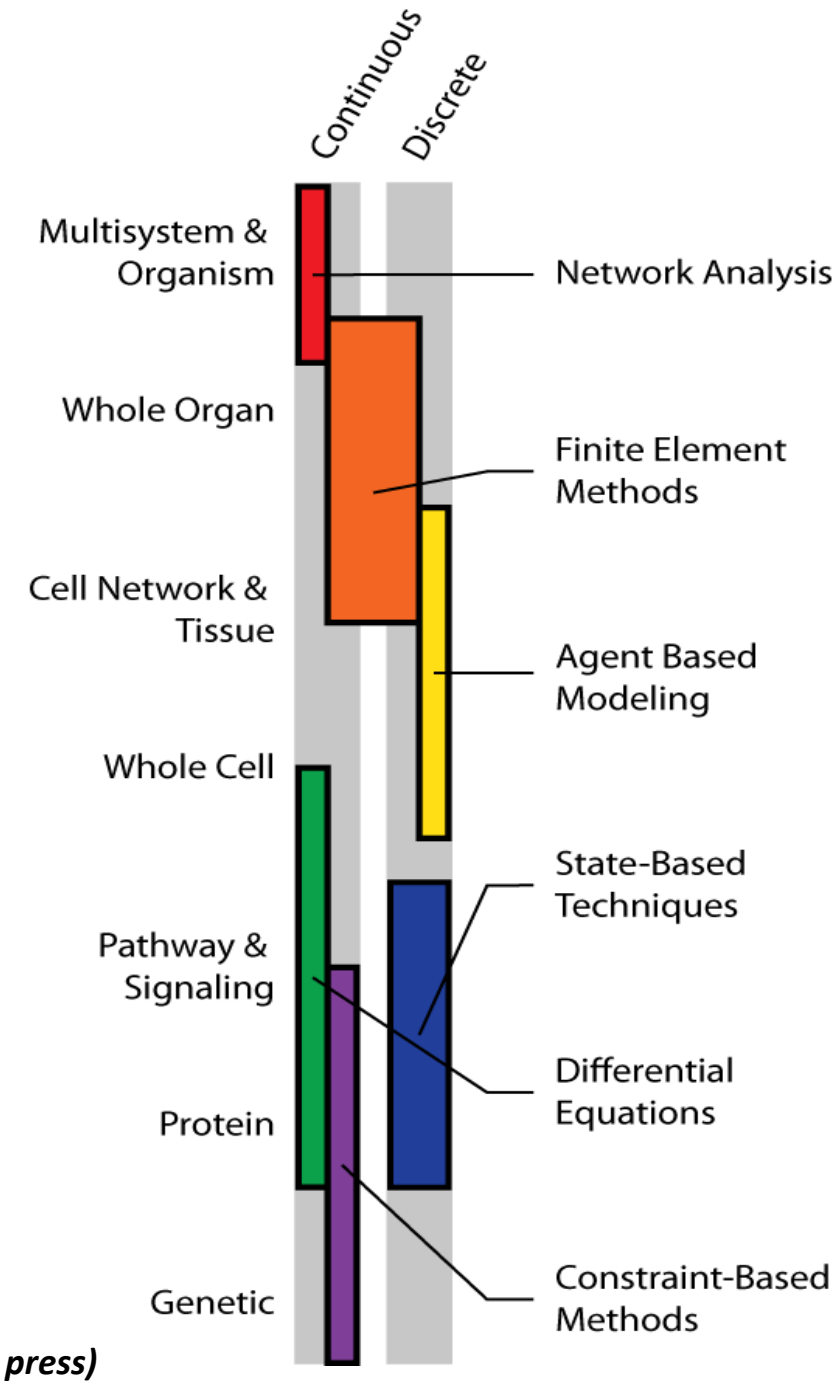

J. Walpole, J.A. Papin, S.M. Peirce (in press)

Multiscale Model Taxonomy

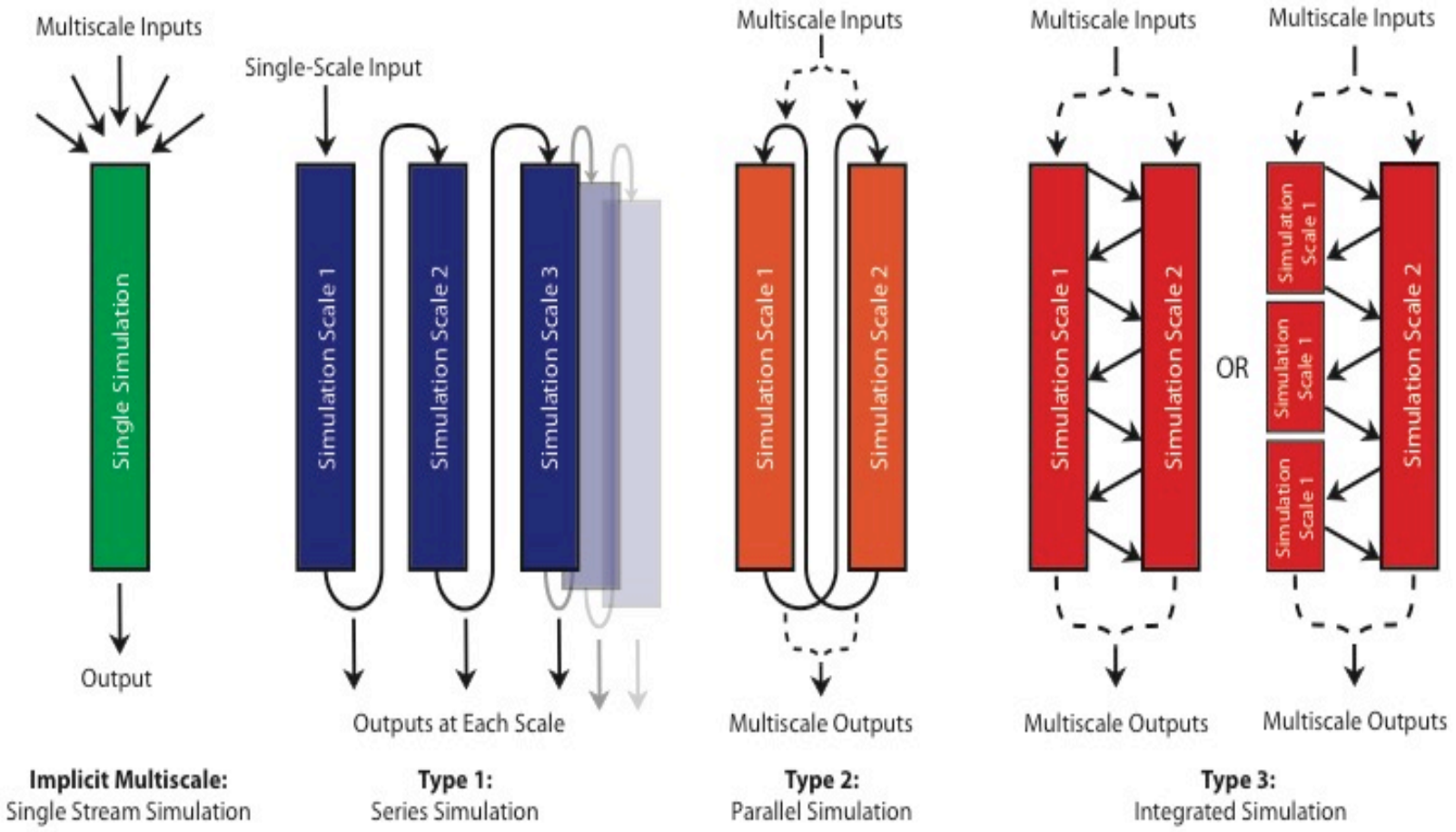

J. Walpole, J.A. Papin, S.M. Peirce (in press)

ABM Bridging to Intracellular

Capillary sprouting in the mouse embryoid body

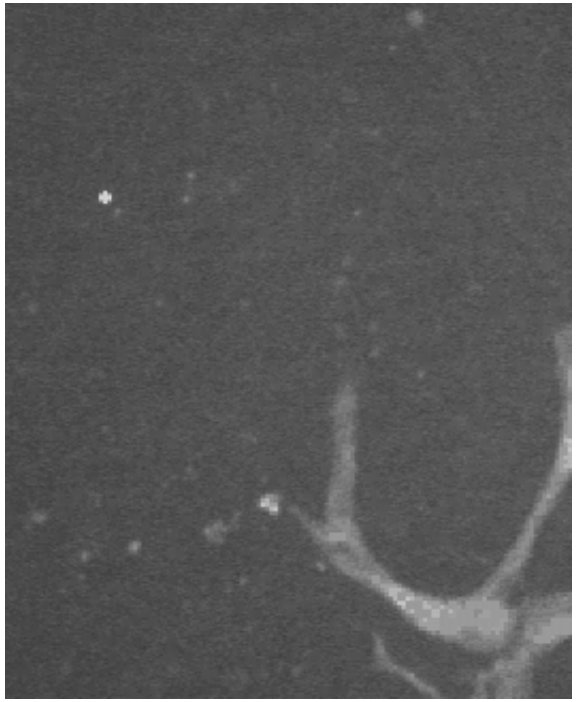

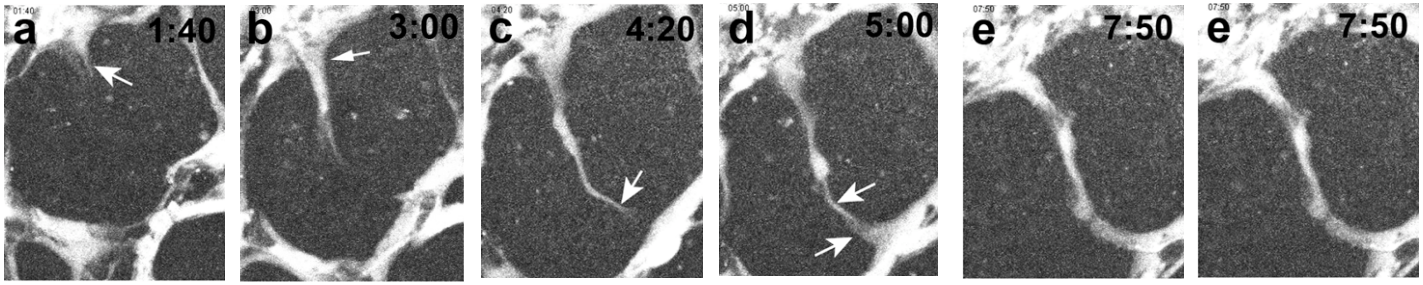

F. Mac Gabhann, S.M. Peirce, V. Bautch (2012)

VEGF-NOTCH

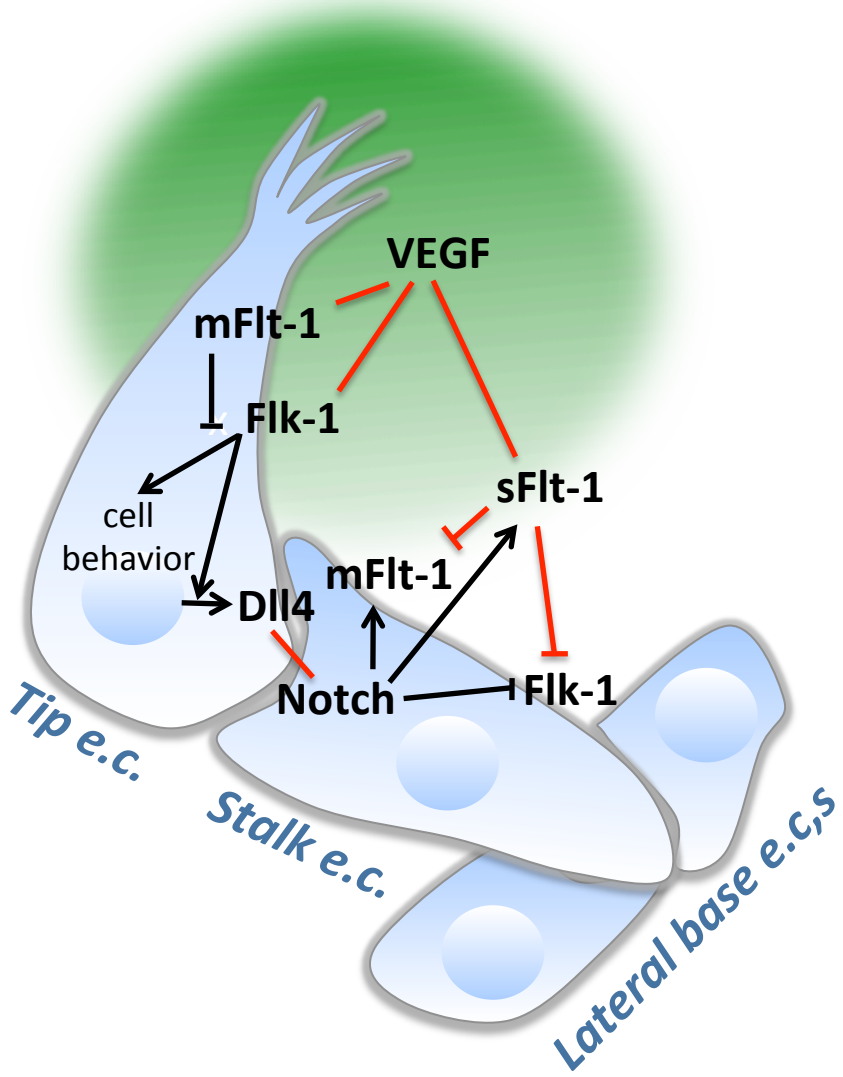

F. Mac Gabhann, S.M. Peirce, V. Bautch (2012)

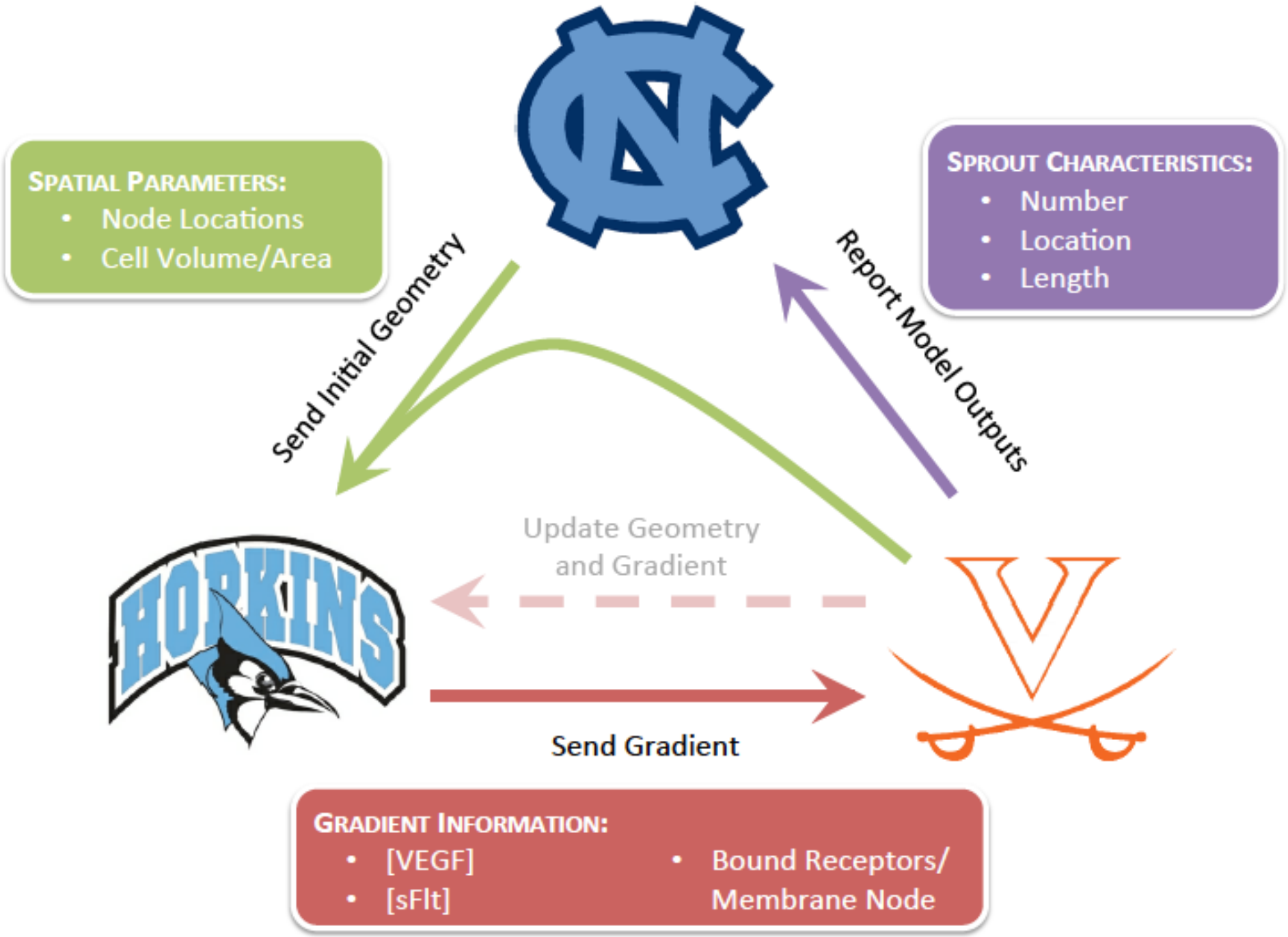
Spatial Parameters:
• Node Locations
• Cell Volume/Area
Sprout Characteristics:
• Number
• Location
• Length
Send Initial Geometry
Report Model Outputs
Update Geometry and Gradient
Send Gradient
Gradient Information:
• [VEGF]
• [sFlt]
• Bound Receptors/ Membrane Node

ABM Initial Geometries

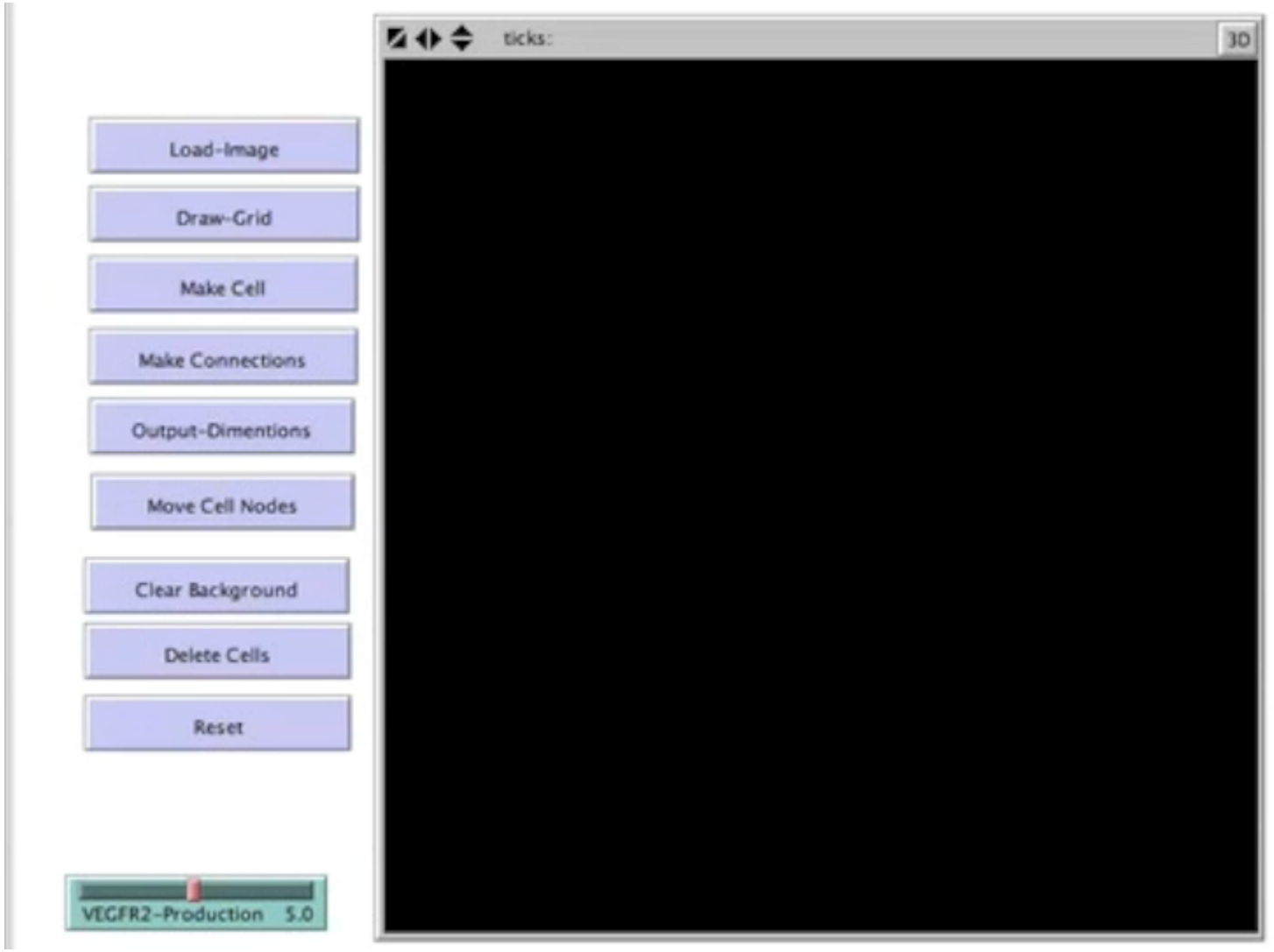

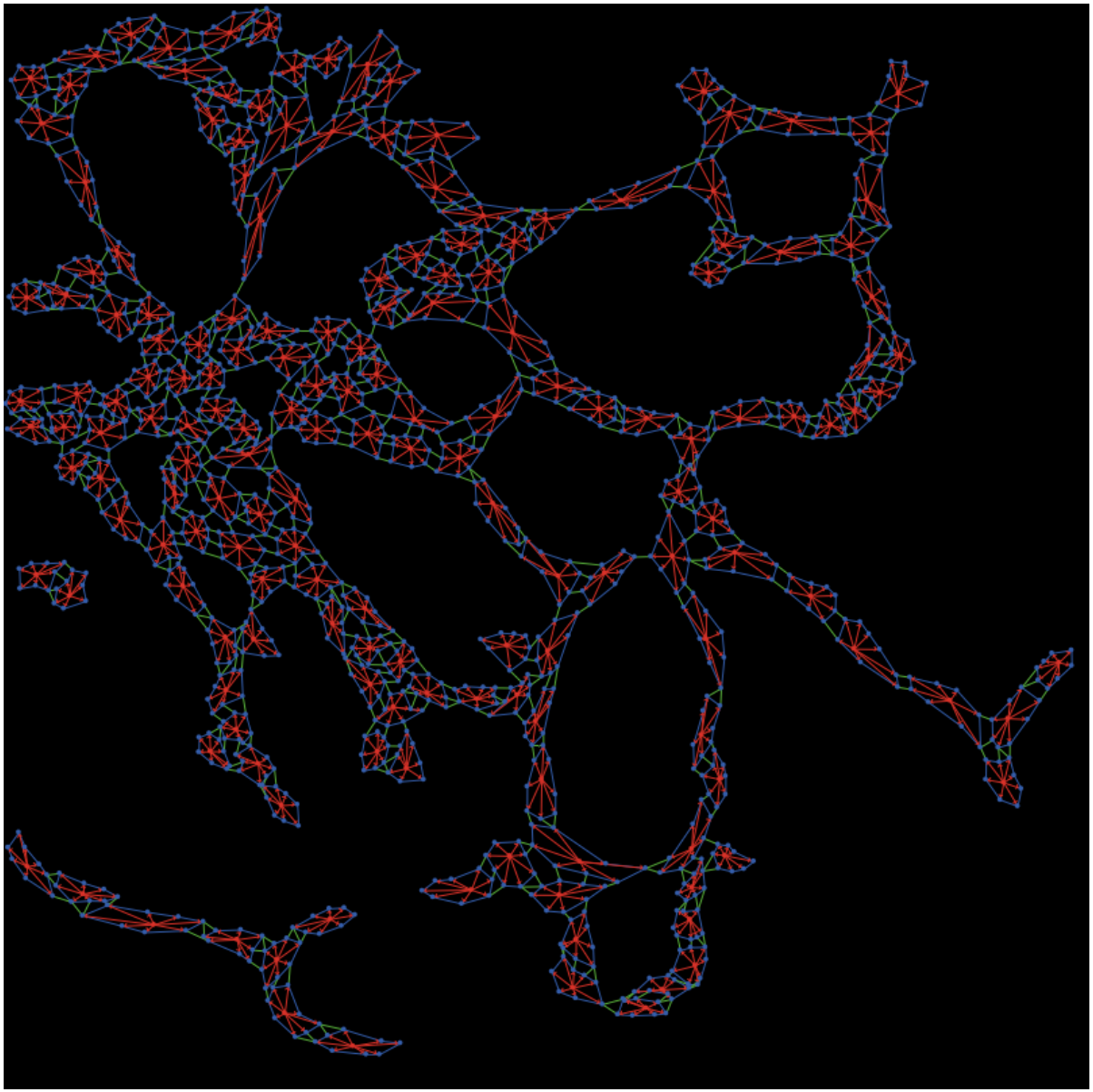

Governing Rules

Embryoid Body

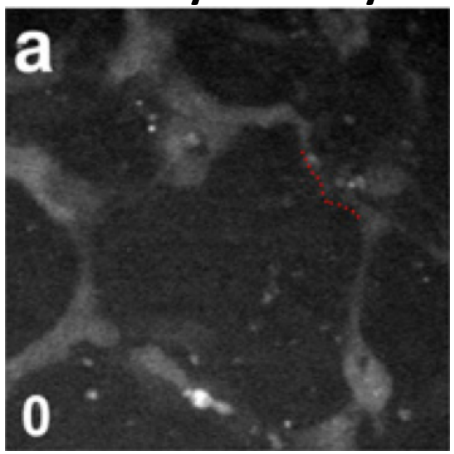

ABM

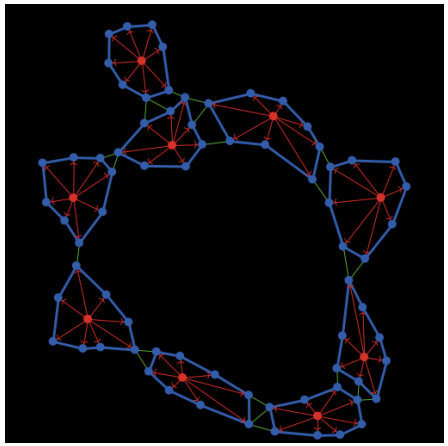

$$qVEGFR2 = qVEGFR2_{min} + (qVEGFR2_{max} - qVEGFR2_{min})e^{-k*Active\_NOTCH}$$

$$\frac{dActive\_NOTCH}{dt} = k_{Activation} * Inactive\_NOTCH * \sum_{cells} DLL4 - k_{deg} * Active\_NOTCH$$

PDE

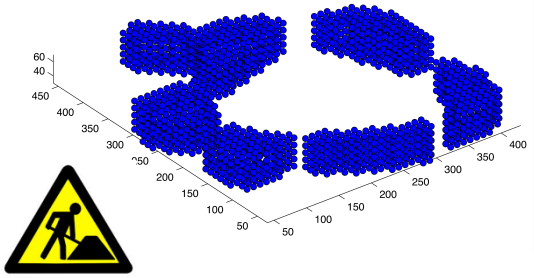

$$\frac{\partial[V]}{\partial t} = q_V + D_V\nabla^2[V] - \sum_i\left(k_{on}[V][M_i] - k_{off}[V\cdot M_i]\right) - \sum_i\left(k_{on}[V][R_j] - k_{off}[V\cdot R_j]\right) - k_{deg}[V]$$

$$\frac{dR}{dt} = s_R - k_{\text{int}\,R} - \sum_i\left(k_{on}[V_i][R] - k_{off}[V_i\cdot R]\right) - \sum_i\left(k_{\text{dim}}[V_i\cdot R][R] - k_{off}[R\cdot V_i\cdot R]\right)$$

PDE: Flk-1 Activation

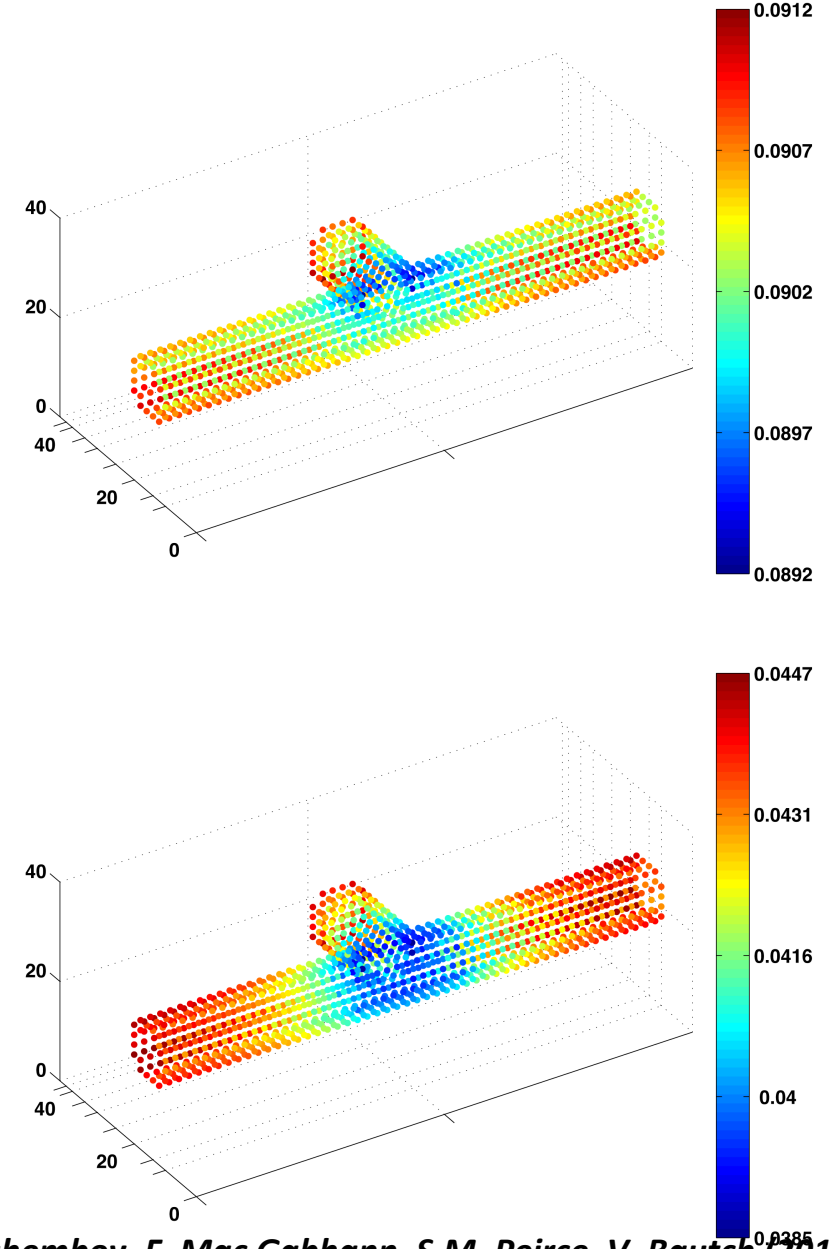

sFlt

mFlt

Tip to base gradient: 2%

sFlt

mFlt

Tip to base gradient: 16%

Y. Hashemboy, F. Mac Gabhann, S.M. Peirce, V. Bautch (2012)

Multiscale Model Workflow

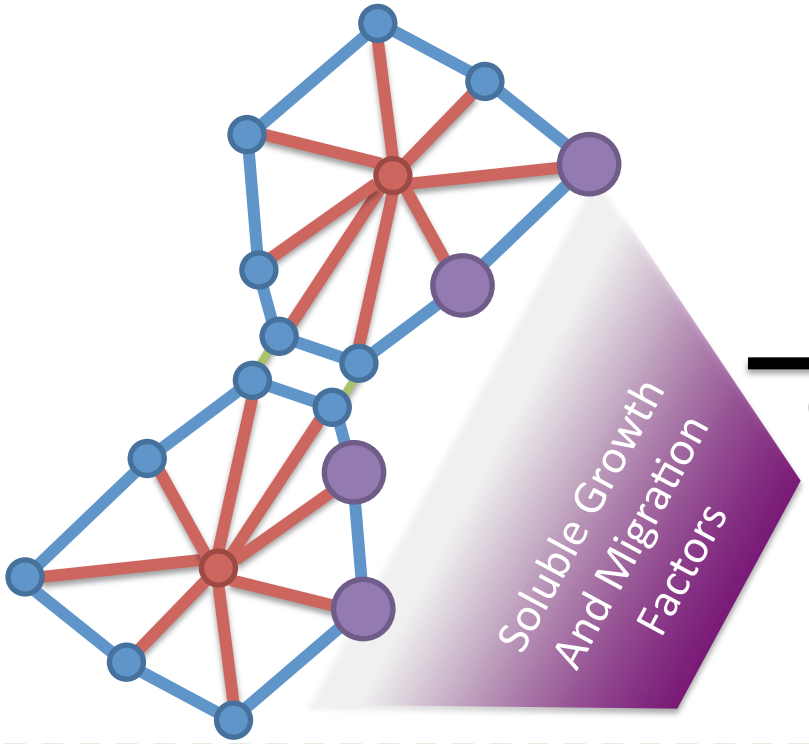

Cell Migration
Mitosis
Apoptosis
Etc.

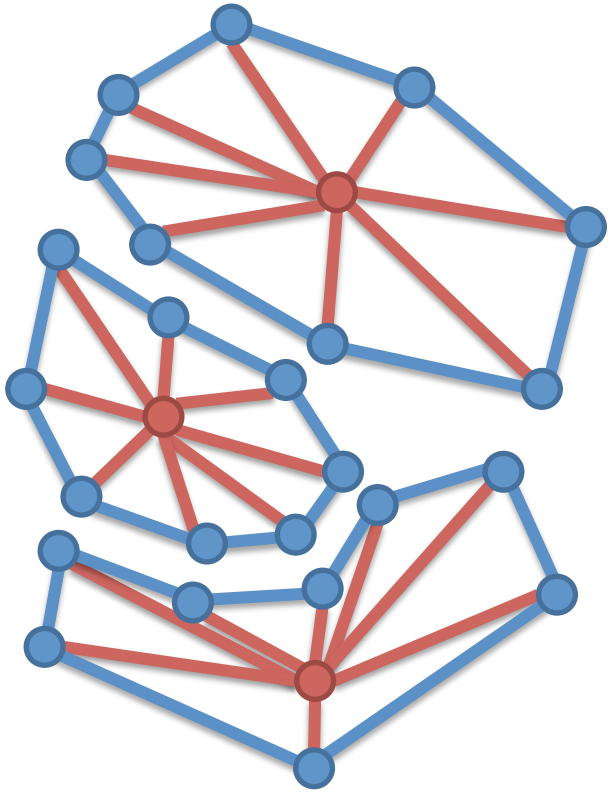

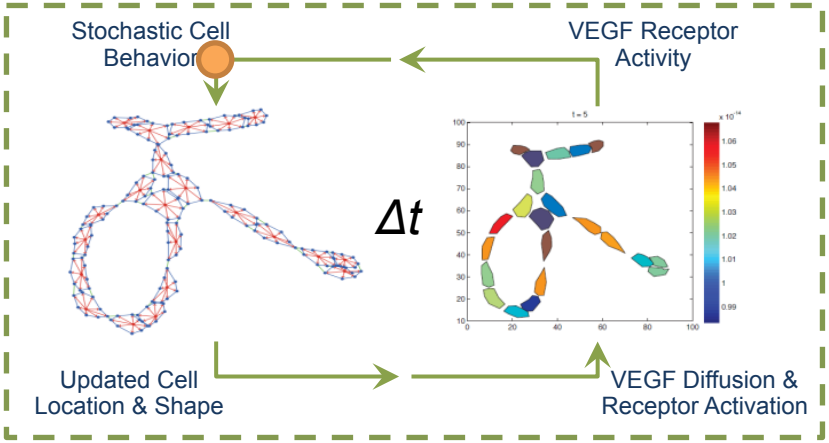

1. Cells **receive signaling cues** from receptor binding inputs
2. Cells **respond with behaviors** such as Migration and Mitotic Cell Division
3. Boundary condition **"landscape" has changed** and require updating

Multiscale Model Workflow

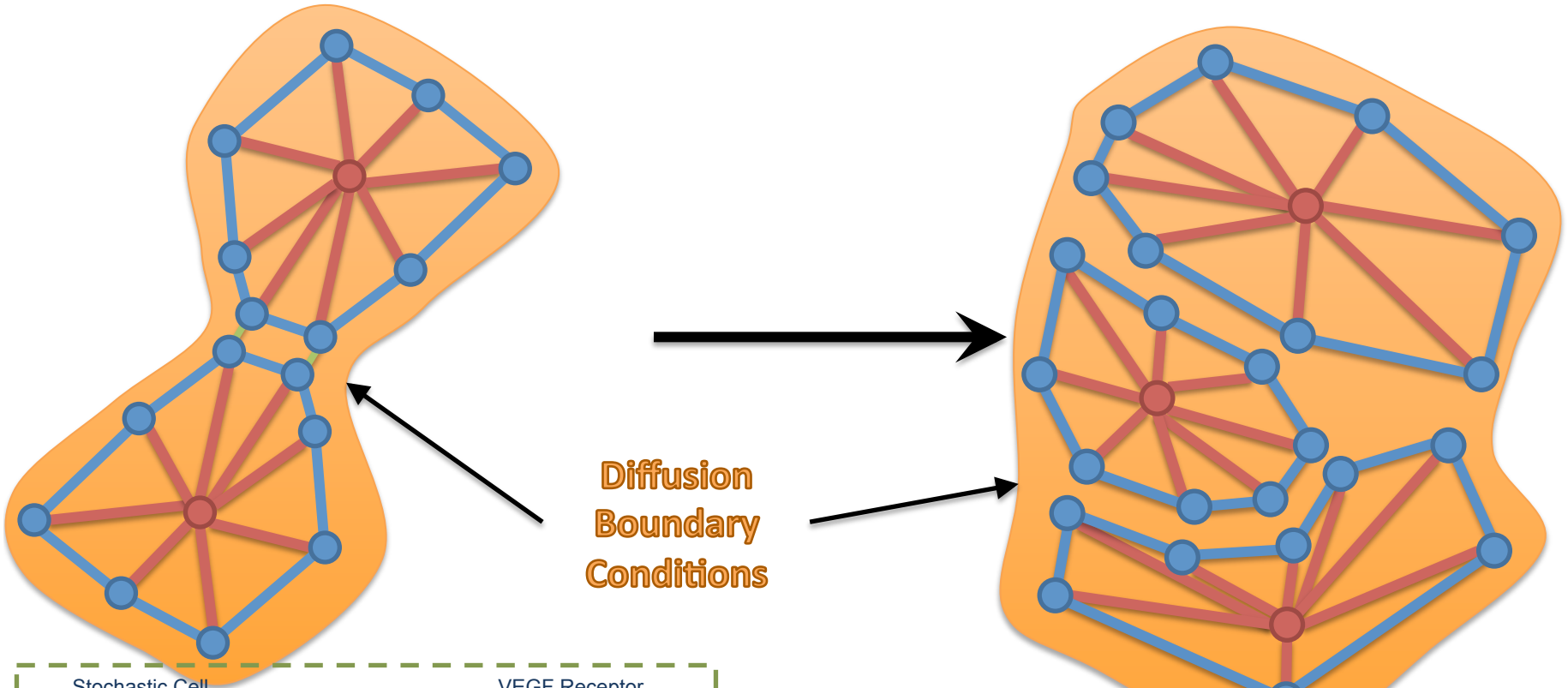

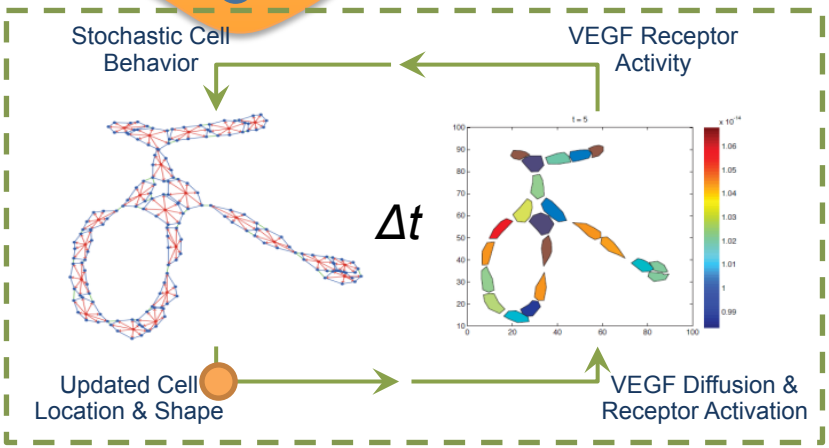

1. Cells **receive signaling cues** from receptor binding inputs
2. Cells **respond with behaviors** such as Migration and Mitotic Cell Division
3. Boundary condition **"landscape" has changed** and require updating

Multiscale Model Workflow

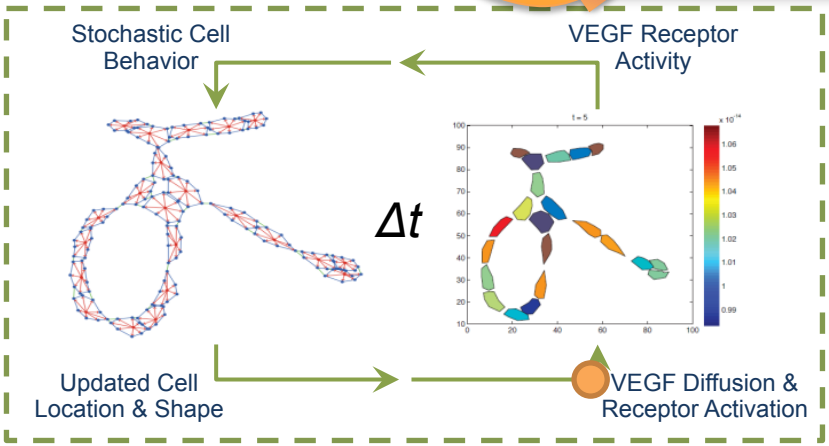

1. **VEGF is produced** and allowed to diffuse based on boundary conditions
2. Receptor binding is determined based on **molecular kinetics**
3. Activated **receptors serve as outputs** to the agent based model

Multiscale Model Workflow

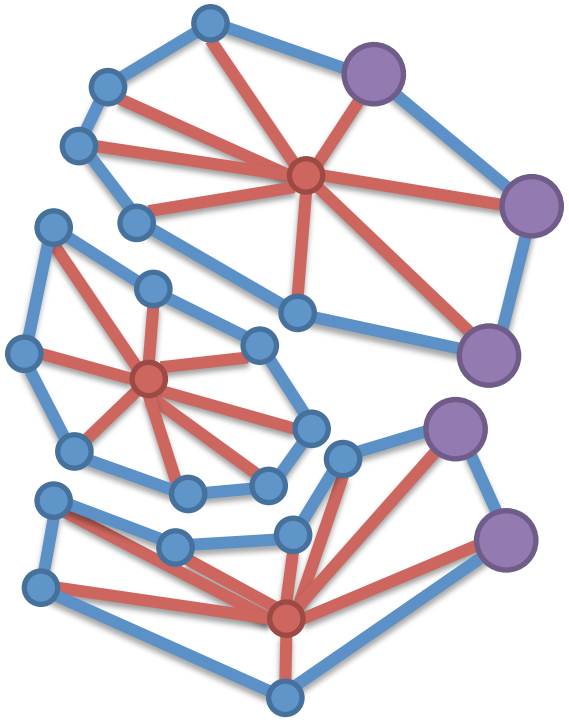

Cell Migration
Mitosis
Apoptosis
Etc.

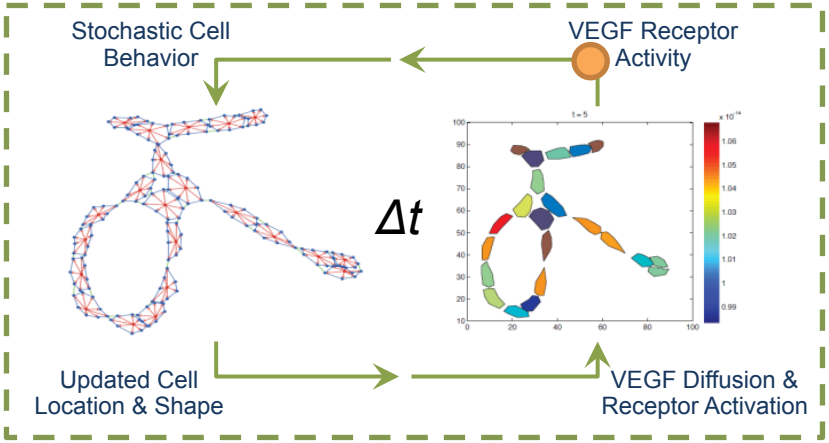

1. Cells **receive signaling cues** from receptor binding inputs
2. Cells **respond with behaviors** such as Migration and Mitotic Cell Division
3. Boundary condition **"landscape" has changed** and require updating

Multiscale Model: Flk-1 Activation

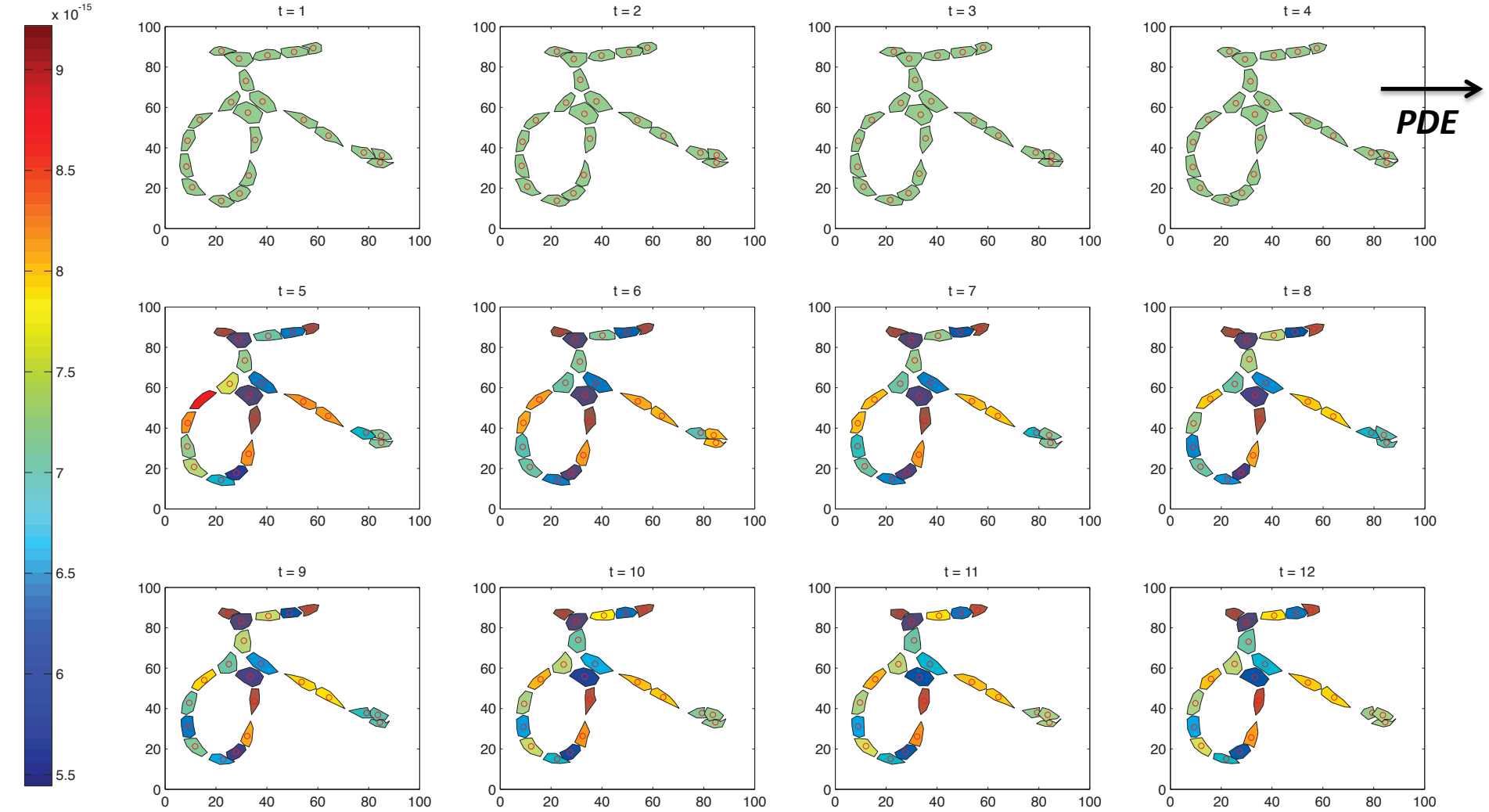

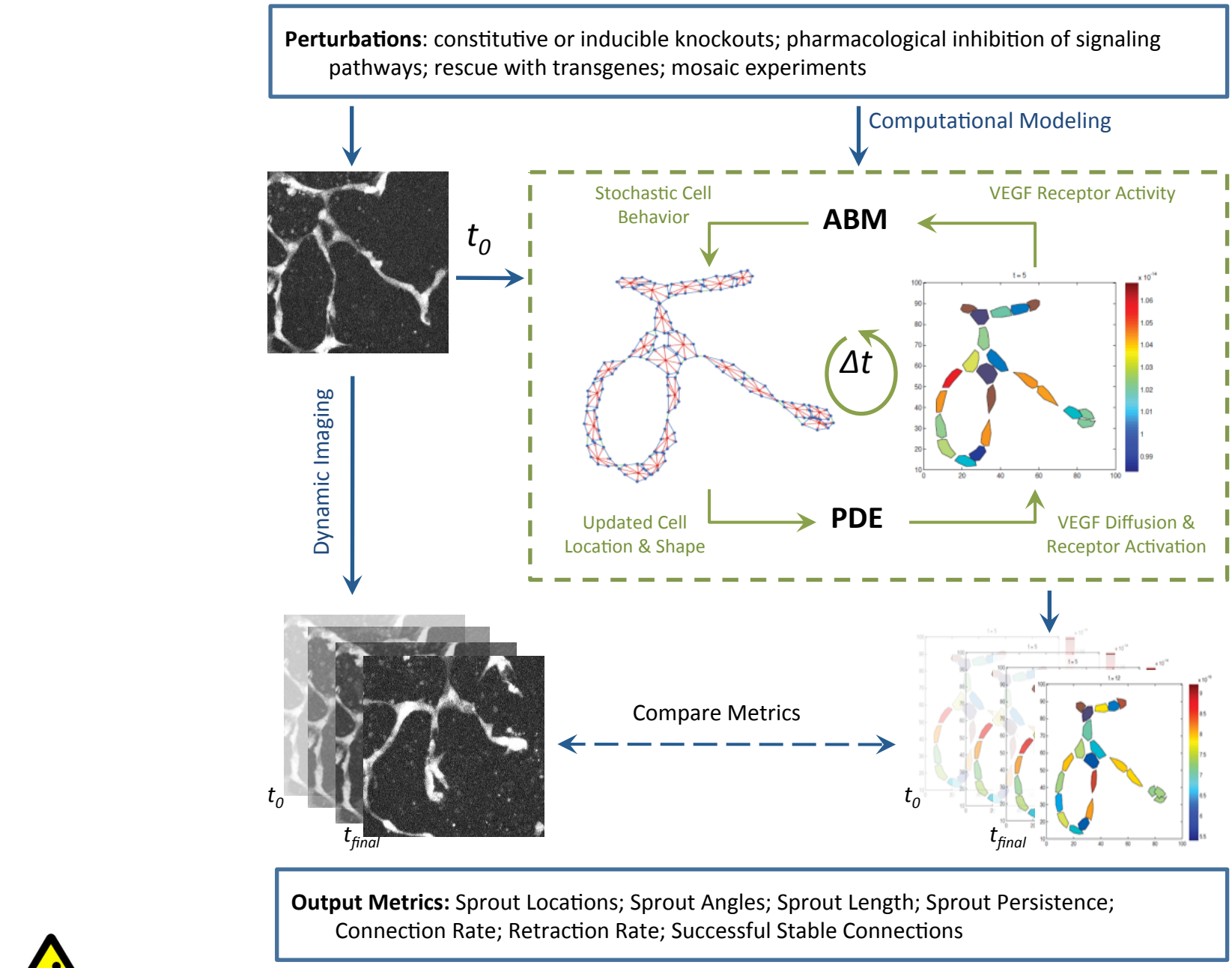
Perturbations: constitutive or inducible knockouts; pharmacological inhibition of signaling pathways; rescue with transgenes; mosaic experiments
Computational Modeling
t_0
Dynamic Imaging
Stochastic Cell Behavior
ABM
VEGF Receptor Activity
Δt
Updated Cell Location & Shape
PDE
VEGF Diffusion & Receptor Activation
Compare Metrics
t_0
t_{final}
t_0
t_{final}
Output Metrics: Sprout Locations; Sprout Angles; Sprout Length; Sprout Persistence; Connection Rate; Retraction Rate; Successful Stable Connections

Multiscale Model Validation

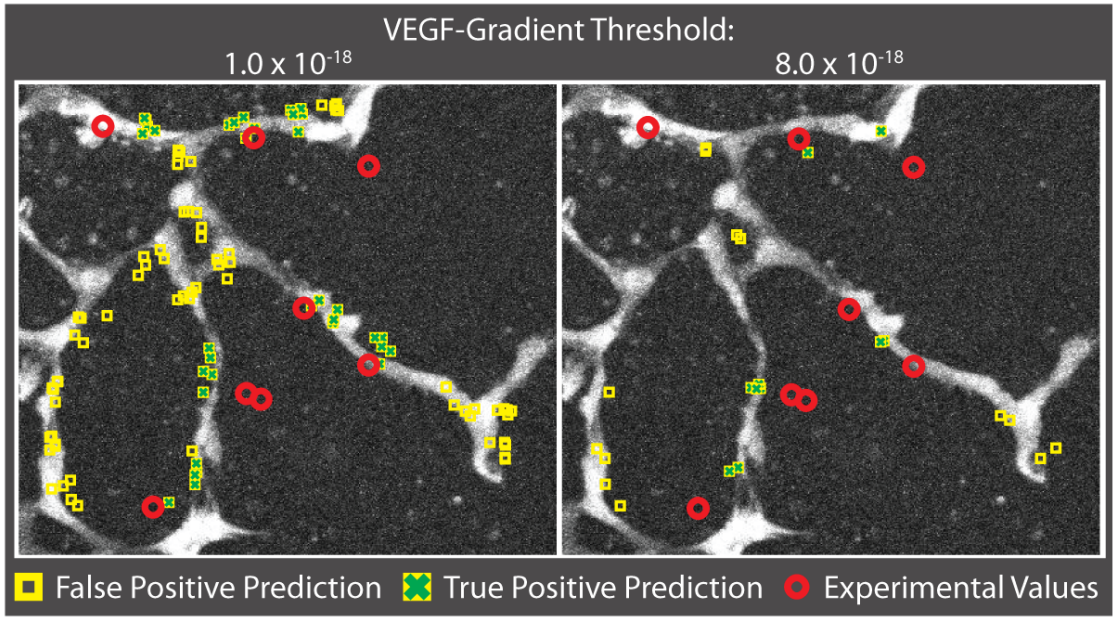

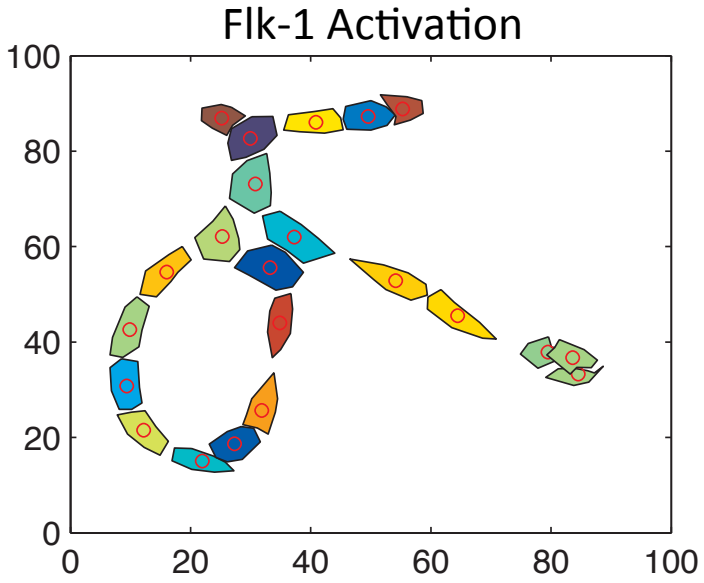

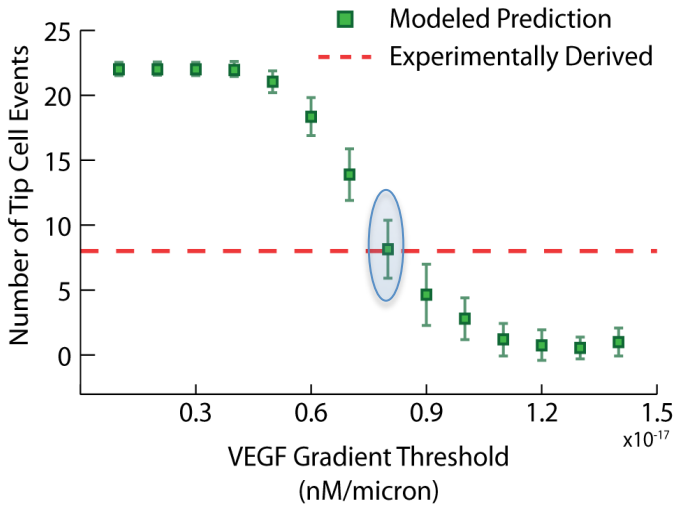

ABM Bridging to Tissue-Level

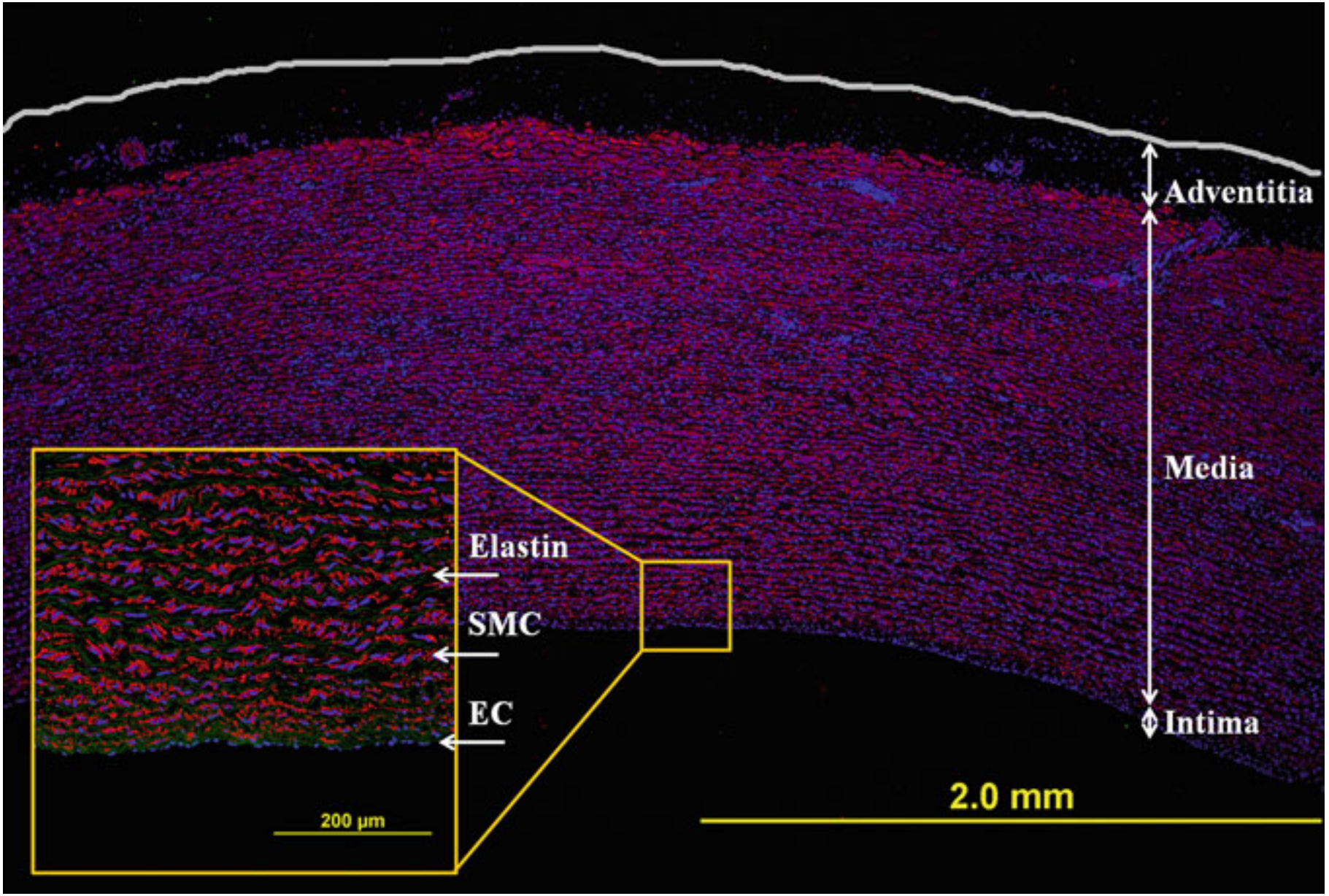

H. Hayenga, B.C. Thorne, P. Yen, J.A. Papin, S.M. Peirce, J.D. Humphrey (2012)

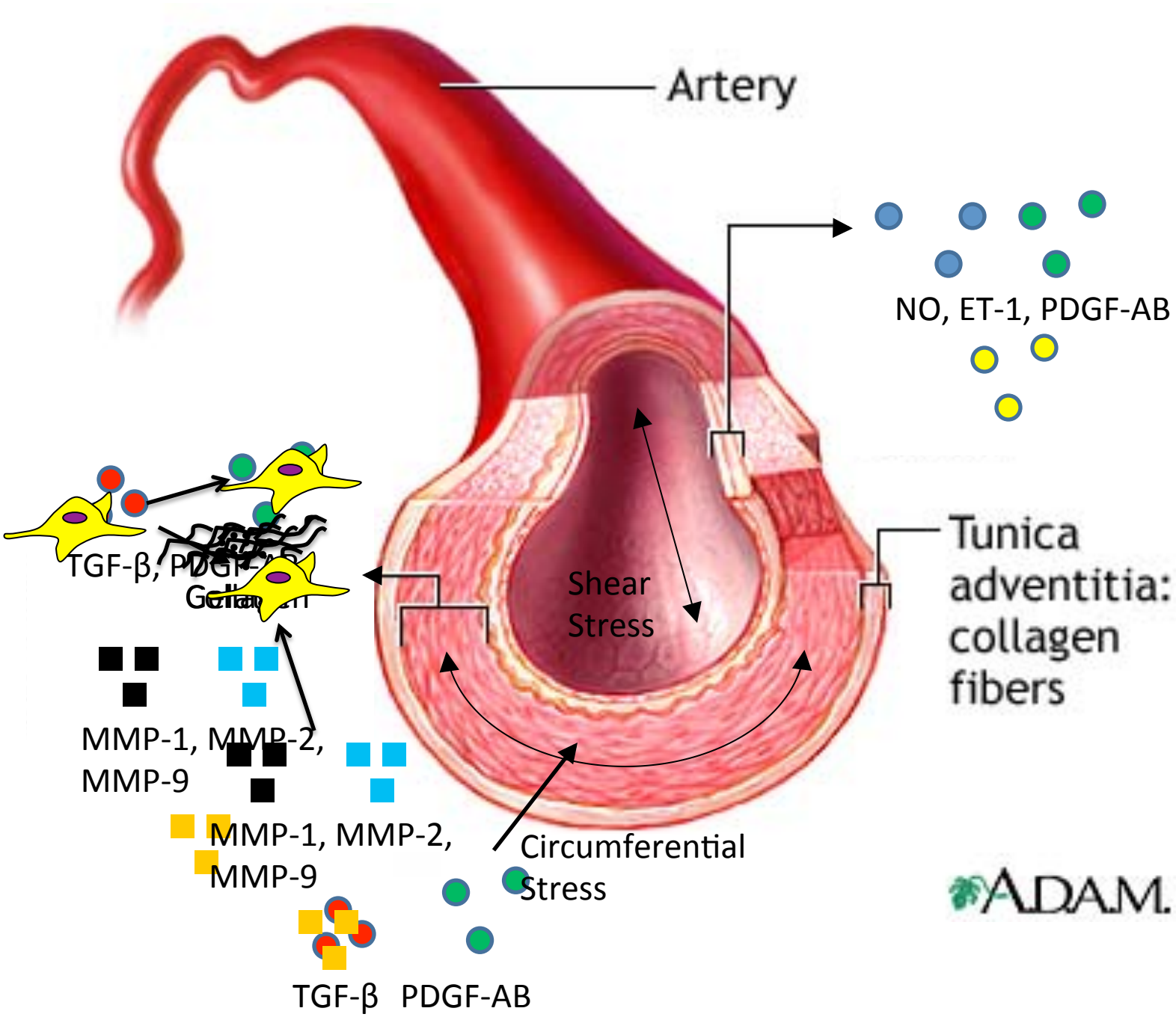
Artery
NO, ET-1, PDGF-AB
TGF-β, PDGF-AB
Collagen
Shear Stress
Tunica adventitia: collagen fibers
MMP-1, MMP-2, MMP-9
MMP-1, MMP-2, MMP-9
Circumferential Stress
TGF-β PDGF-AB
A.D.A.M.

Multiscale Model

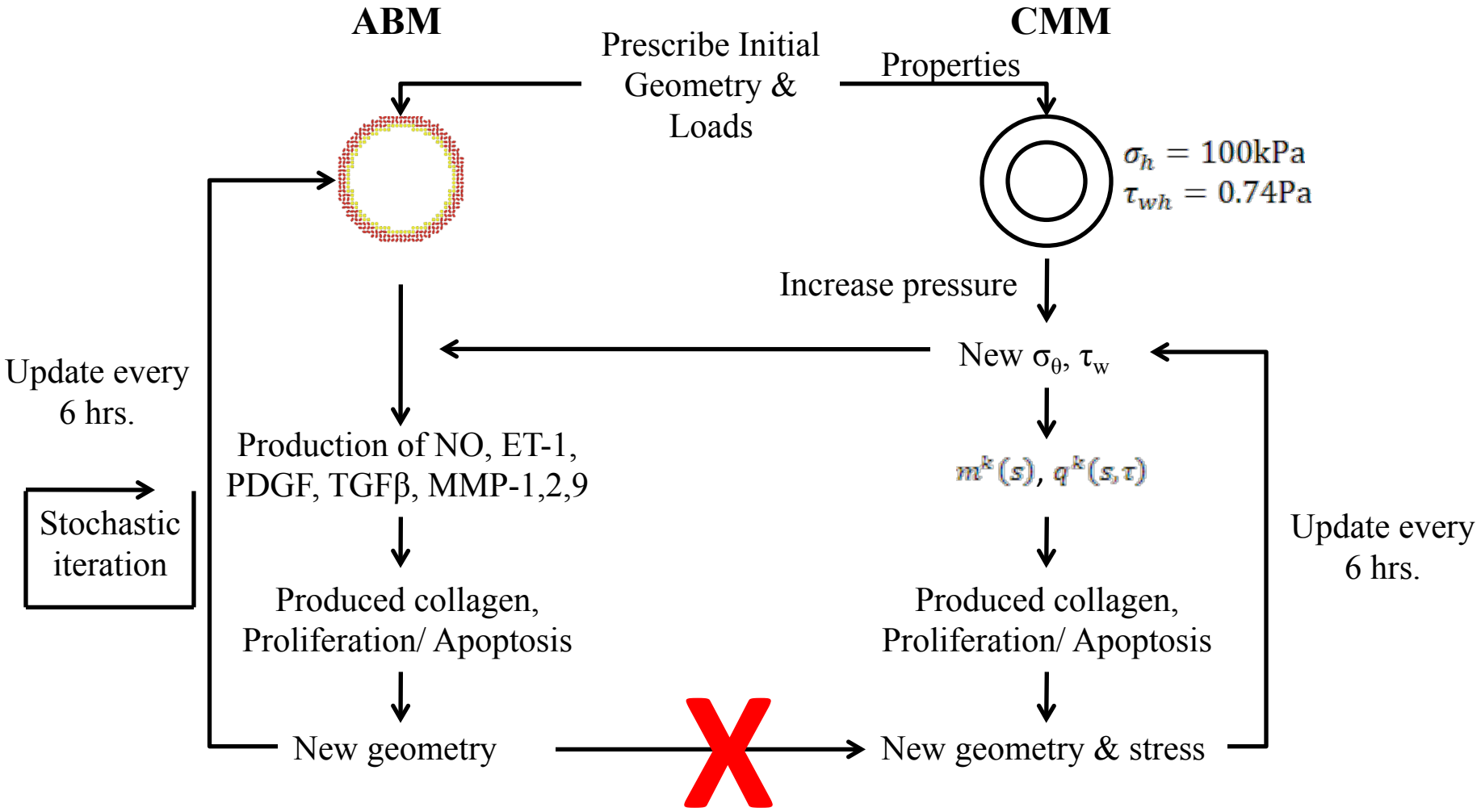

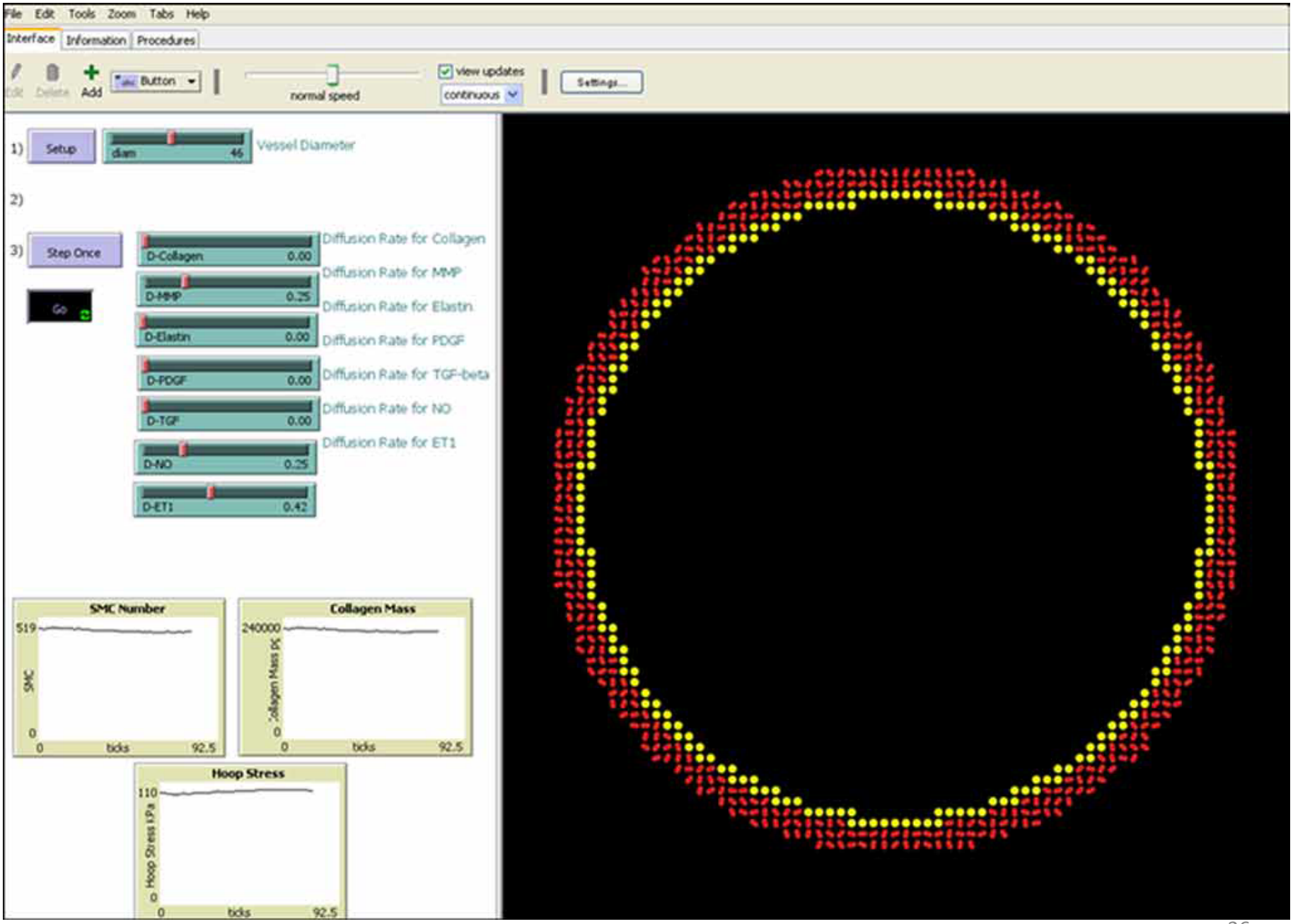

B.C. Thorne, H. Hayenga, J.D. Humphrey, S.M. Peirce (2011)

Objective Function:

$$e = \frac{2}{N}\sum_{j}^{N}\left(\frac{\left|C_{NT}^{ABM} - C_{NT}^{CMM}\right|}{C_{NT}^{ABM} + C_{NT}^{CMM}} + \frac{\left|M_{NT}^{ABM} - M_{NT}^{CMM}\right|}{M_{NT}^{ABM} + M_{NT}^{CMM}}\right)_j + \frac{2}{S}\sum_{j}^{S}\left(\frac{\left|C_{HT}^{ABM} - C_{HT}^{CMM}\right|}{C_{HT}^{ABM} + C_{HT}^{CMM}} + \frac{\left|M_{HT}^{ABM} - M_{HT}^{CMM}\right|}{M_{HT}^{ABM} + M_{HT}^{CMM}}\right)_j$$

TABLE 2. Listed are both the initial values of the parameters and the bounds that defined the search space used in the genetic algorithm to improve congruency between ABM and CMM predictions of smooth muscle and collagen mass via Eq. (5).

Parameter	Initial value	Lower bound	Upper bound	After genetic algorithm
$K_{\sigma_\theta}^{c}$	1	0.1	10	1.11
$K_{\sigma_\theta}^{m}$	10	0.1	10	3.85
$K_{\tau_w}^{c}$	1	0.1	10	2.85
$K_{\tau_w}^{m}$	10	0.1	10	8.75
$MMP\text{-}1_0$	2.69E−04	2.69E−05	2.69E−03	9.47E−04
$MMP\text{-}1_{\%A}$	0.39	0.039	3.93	1.04
C_0	0.009	0.0009	0.09	0.07
C_{TGF}	114.94	11.49	1149.42	134.57
M_p	−1.45E+09	−1.45E+10	−9.69E+08	−1.53E+09
M_0	80,000	53333.33	120,000	6.12E+04
M_{a1}	71020	7102	106530	9.89E+04
M_{a2}	100	66.66	1000	223.21
$PDGF_{\sigma_\theta}$	4.79E−07	3.19E−07	7.19E−07	7.03E−07
$PDGF_0$	4.17E−05	4.17E−06	6.25E−05	6.17E−05
$TGF\beta_{\sigma_\theta}$	1.65E−06	1.65E−07	1.65E+05	7.87E−06
$TGF\beta_0$	1.03E−04	1.03E−05	1.03E−03	3.69E−04

Note that 16 parameters were allowed to vary: CMM (top 4 rows) and ABM (bottom 12 rows). See Eqs. (1) and (2), Appendix, and Table 1 in Thorne *et al.*[37] for associated constitutive equations, definitions, or rules. Also listed are the final values of the parameters following minimization.

H. Hayenga, B.C. Thorne, S.M. Peirce, J.D. Humphrey (2011)

ABM Prediction

Normotensive

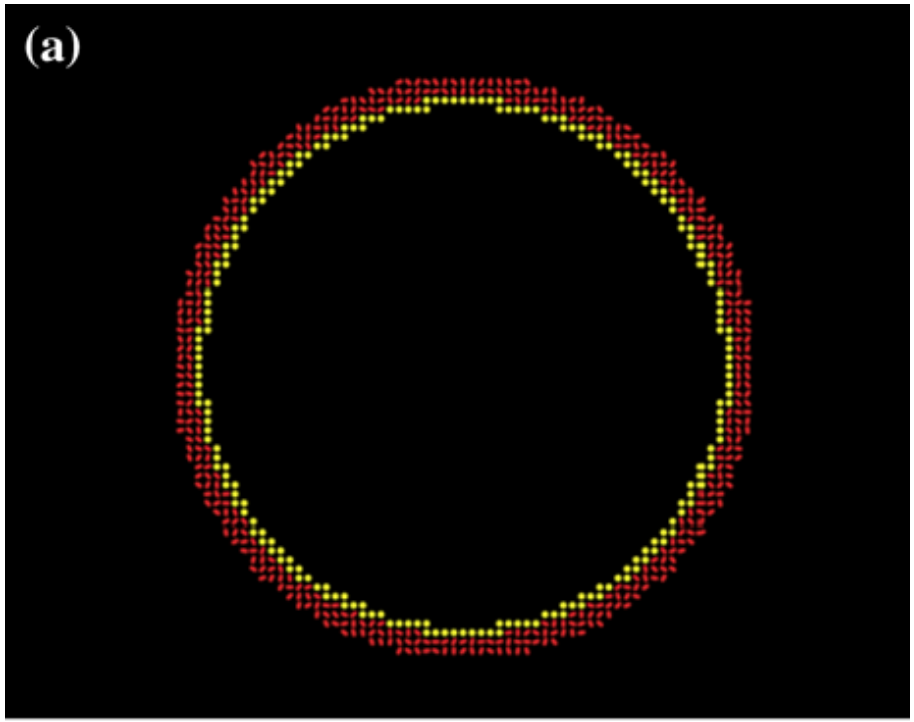

Hypertensive

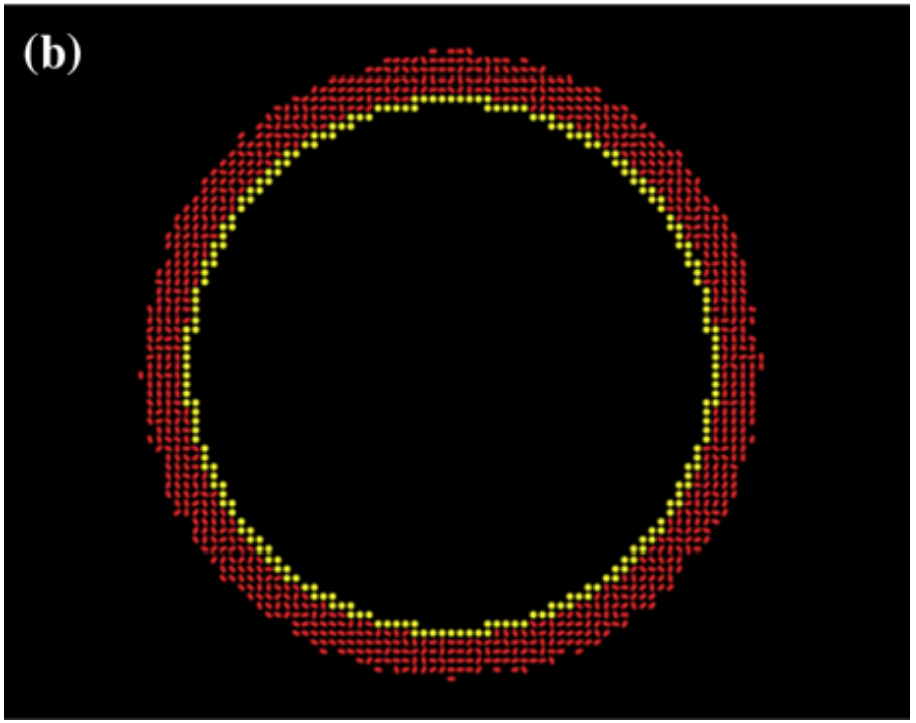

H. Hayenga, B.C. Thorne, S.M. Peirce, J.D. Humphrey (2011)

No congruency check

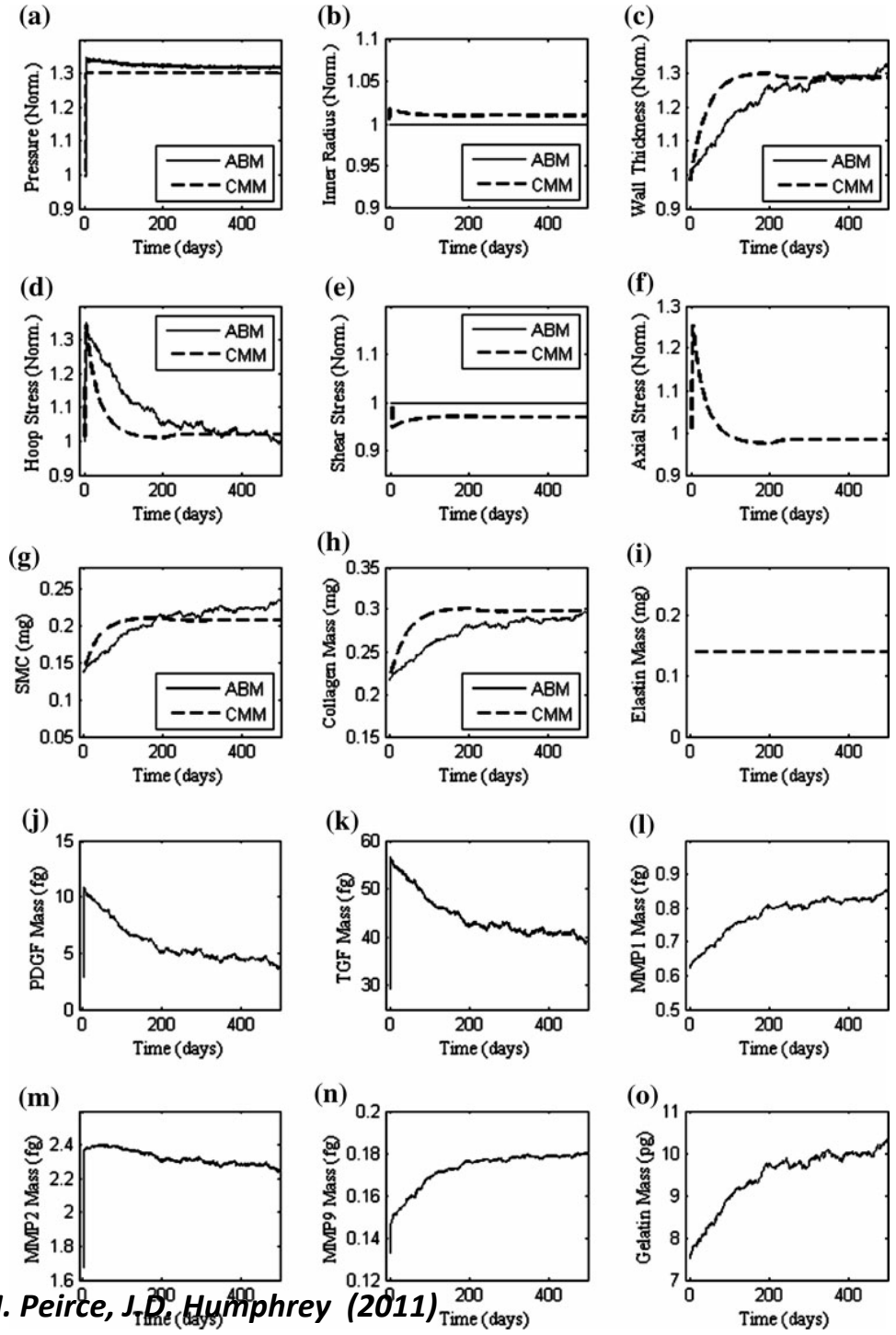

H. Hayenga, B.C. Thorne, S.M. Peirce, J.D. Humphrey (2011)

With congruency check

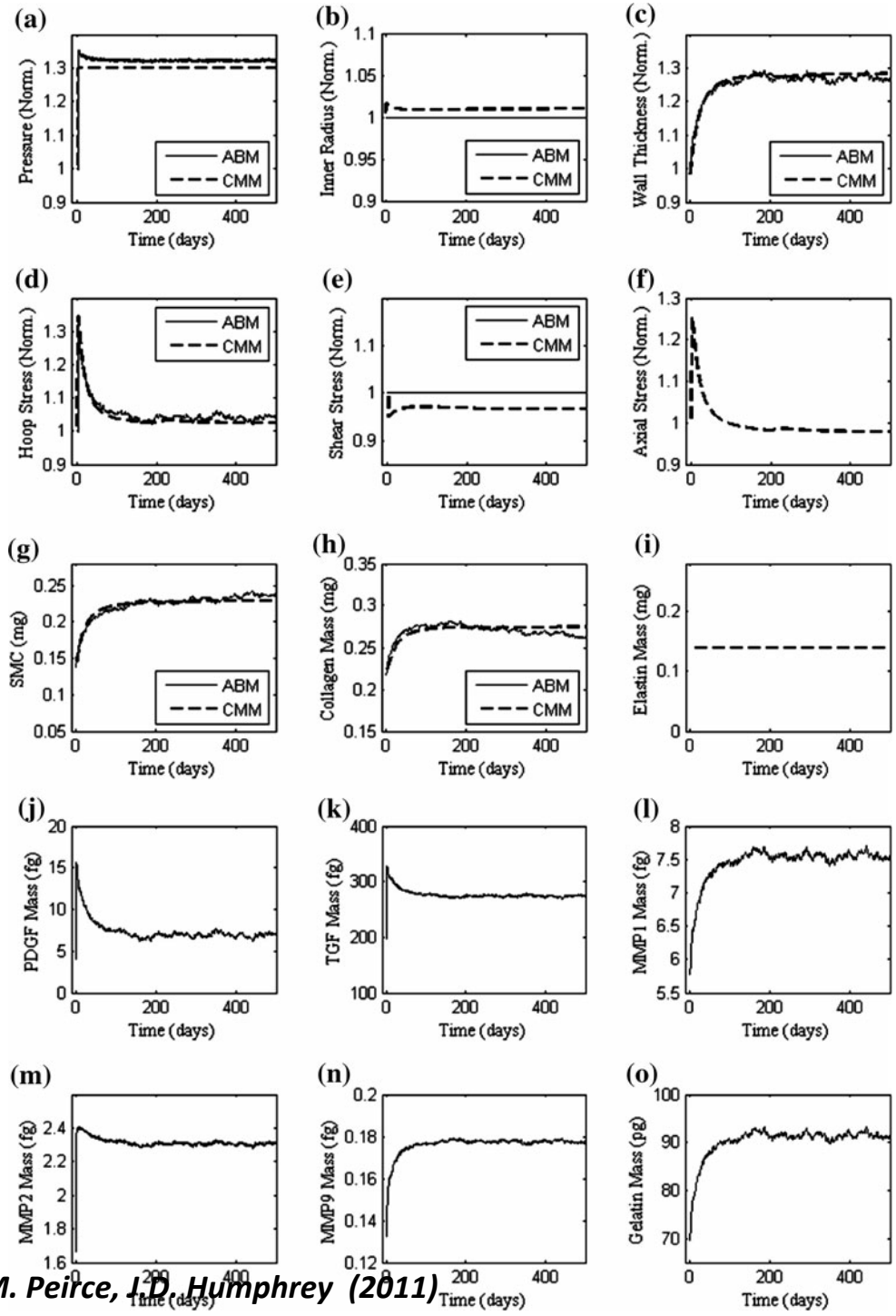

H. Hayenga, B.C. Thorne, S.M. Peirce, J.D. Humphrey (2011)

With congruency check of different input

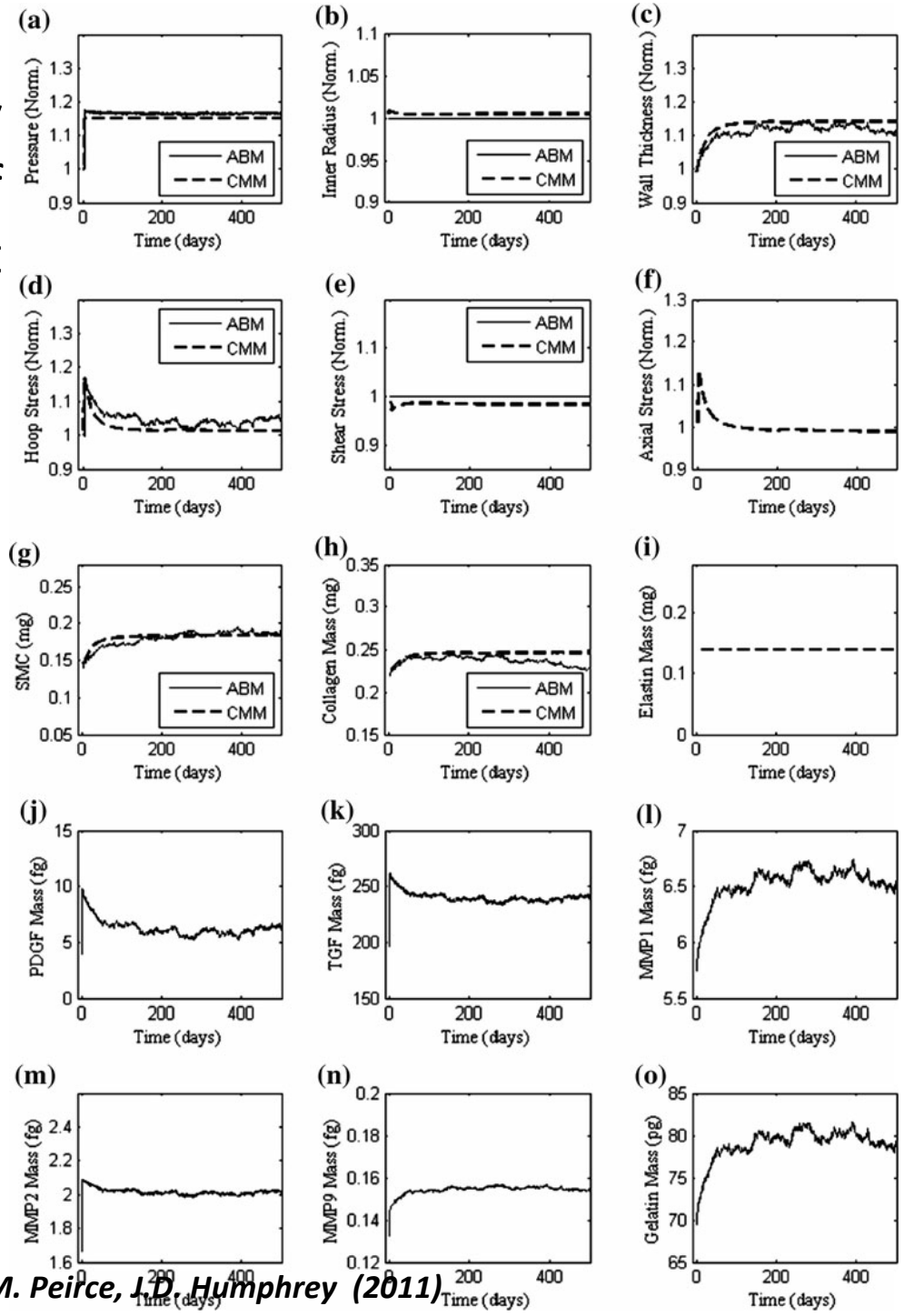

H. Hayenga, B.C. Thorne, S.M. Peirce, J.D. Humphrey (2011)

With congruency check (normotensive)

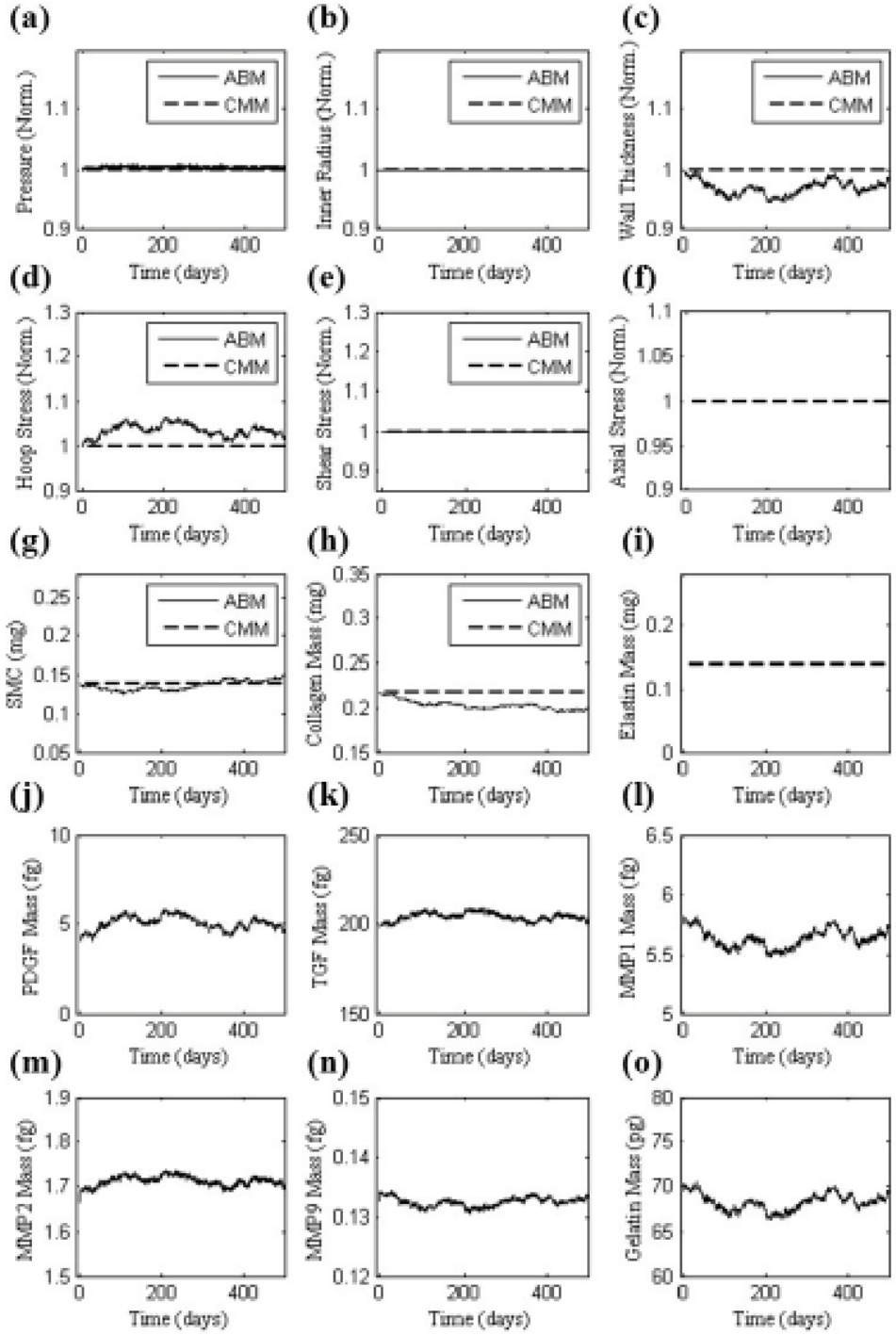

Model Validation

Experiment	Return to normal wall stress	Citation
Systolic pressure increase of 24% in rats	140 days	Wolinsky (1972)
Systolic pressure increase of 30% in rats	126 day	Matsumoto & Hayashi (1994)

Model	Return to normal wall stress
CMM Systolic pressure increase of 30% in mouse	70 days
ABM Systolic pressure increase of 30% in mouse	350 day
With congruency (both ABM and CMM)	125

Summary

Confidence Scoring of ABM Rules

1. ARTICLE AGREEMENT

0 = 0

1 or 2 = 5

3 or 4 = 7

5 or 6 = 9

7 and above = 10

2. PHYSIOLOGICAL METHODS

In vivo, non-linear, residual, anisotropy, heterogeneity accounted for = 10

Ex vivo, pre-conditioned, acute testing, comp. sound = 8

Ex vivo, cultured, pre-conditioned, comp. sound = 6

In vitro, acute testing, environment sound = 4

In vitro, culture = 2

3. SIMILARITY

Cell type: endothelial or SMC = 10; all others = 0

Organ system: arterial = 10; other vessels or organs = 0

Species: mouse = 10; all others = 0

Environmental conditions: *in vivo* = 10; all others = 0*

4. DATA TYPE

Numerical = 10

Theoretical = 6

Descriptive = 2

Measured directly = 10; protein determination by absorbance, electrophoresis

Measured indirectly = 6; amount inferred through the magnitude of fluorescence/stain intensity

Extrapolated = 4

Descriptive = 2

B.C. Thorne, H. Hayenga, J.D. Humphrey, S.M. Peirce (2011)

Confidence Scoring of ABM Rules

Rule	SMC production of PDGF-AB (stress dependent)			
	Researcher 1		Researcher 2	
Relevant papers	Li et al. (1995)	Ma et al. (1999)	Li et al. (1995)	Ma et al. (1999)
1. Article agreement	0	7	5	5
2. Physiological methods	6	4	6	6
3a. Same species	0	0	0	0
3b. Same organ	10	10	10	10
3c. Same cell type	10	10	10	10
3d. Same *in vivo* state	5	5	10	10
3. Similarity metric total:	6.25	6.25	7.5	7.5
4a. Numerical	10	10	10	10
4b. Measured directly	7	7	5	5
4c. Many data points	2	4	2	2
4. Data type total	6.33	7	5.67	5.67
Average confidence	4.65	6.06	6.04	6.04
Composite score	5.36		6.04	

B.C. Thorne, H. Hayenga, J.D. Humphrey, S.M. Peirce (2011)

Hunt et al. Theoretical Biology and Medical Modelling 2011, 8:35
http://www.tbiomed.com/content/8/1/35

THEORETICAL BIOLOGY AND MEDICAL MODELLING

REVIEW Open Access

Relational grounding facilitates development of scientifically useful multiscale models

C Anthony Hunt[1*], Glen EP Ropella[2], Tai ning Lam[3] and Andrew D Gewitz[4]

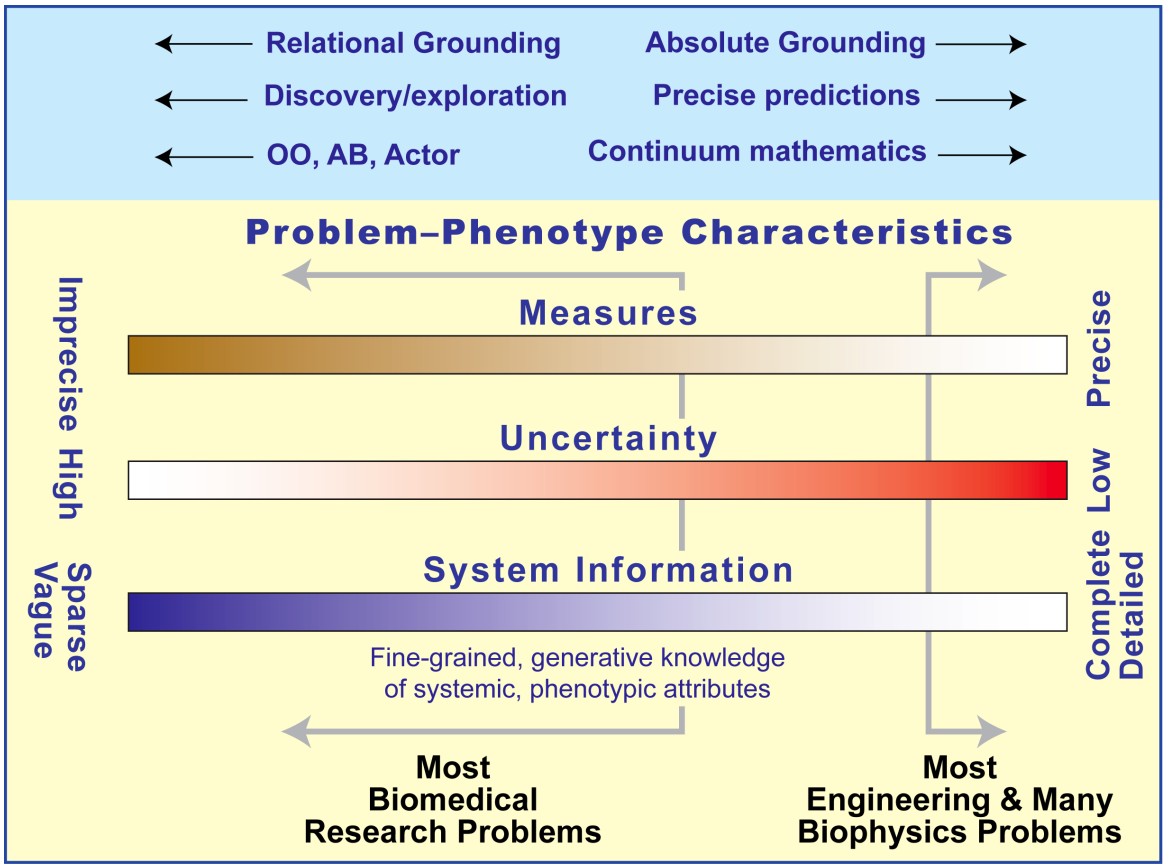

Utility of Computational Modeling

- **Identify key parameters** *(Drug target identification)*
- **Quantitatively pinpoint voids in understanding** *(Mechanism of action)*
- **Compare alternative hypotheses** *(Combination therapies)*
- **Suggest and refine new hypotheses** *(Determine side effects & compensatory pathways)*
- **Calculate what can't be measured** *(Predict dosing and potency)*

Accelerate discovery process

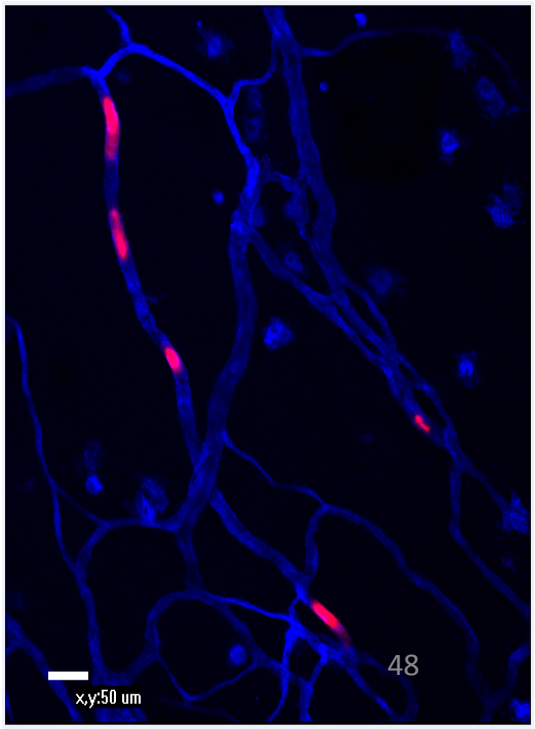

Utility of Multiscale Modeling

In our experience…

- Requires close collaboration & trust
- Conceptual challenges > computational challenges
- Experimental validation is no less important but it is easier?
- Model simplification strategies and choice of parameters in one model can impact predictions of the other
  - ✓ Sensitivity analysis is important
  - ✓ Internal validity checking
  - ✓ Validation against experimental data

Future Work

Multiscale FE and ABM that predicts muscle tissue adaptation to surgery

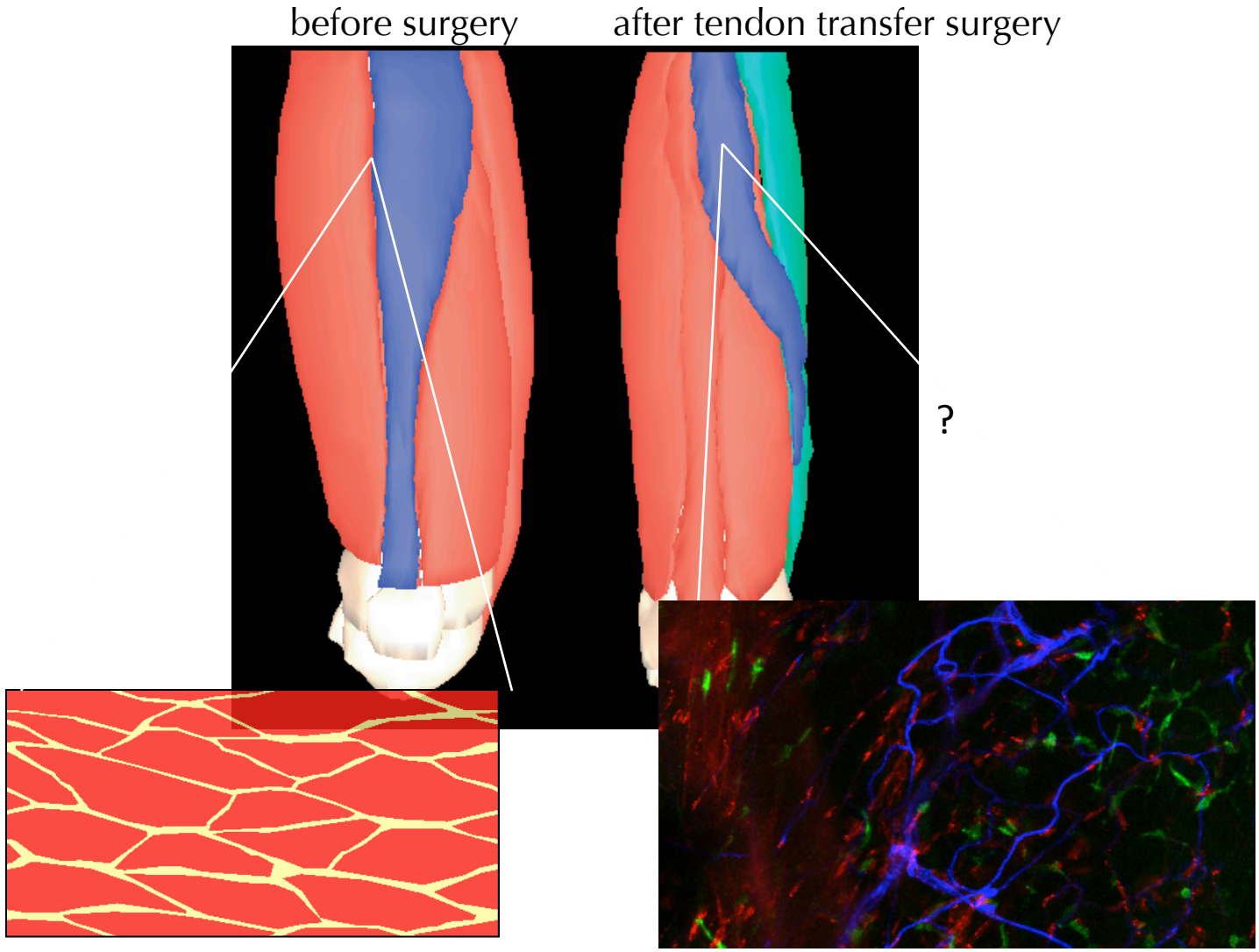

S. Blemker

Multiscale FE and ABM that predicts muscle tissue adaptation to surgery

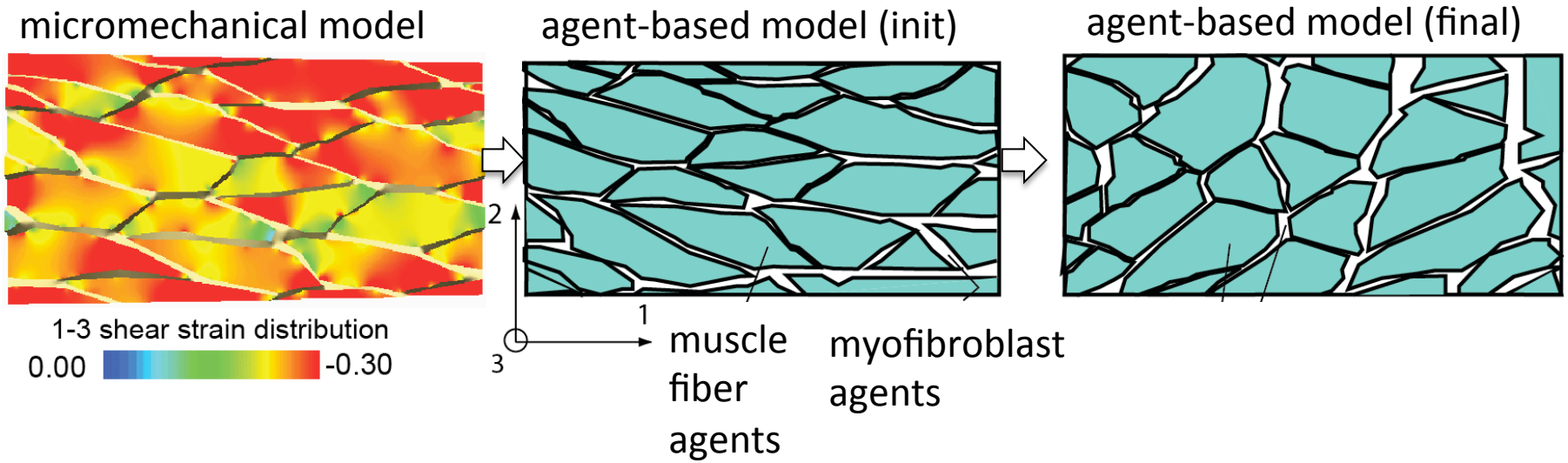

S. Blemker

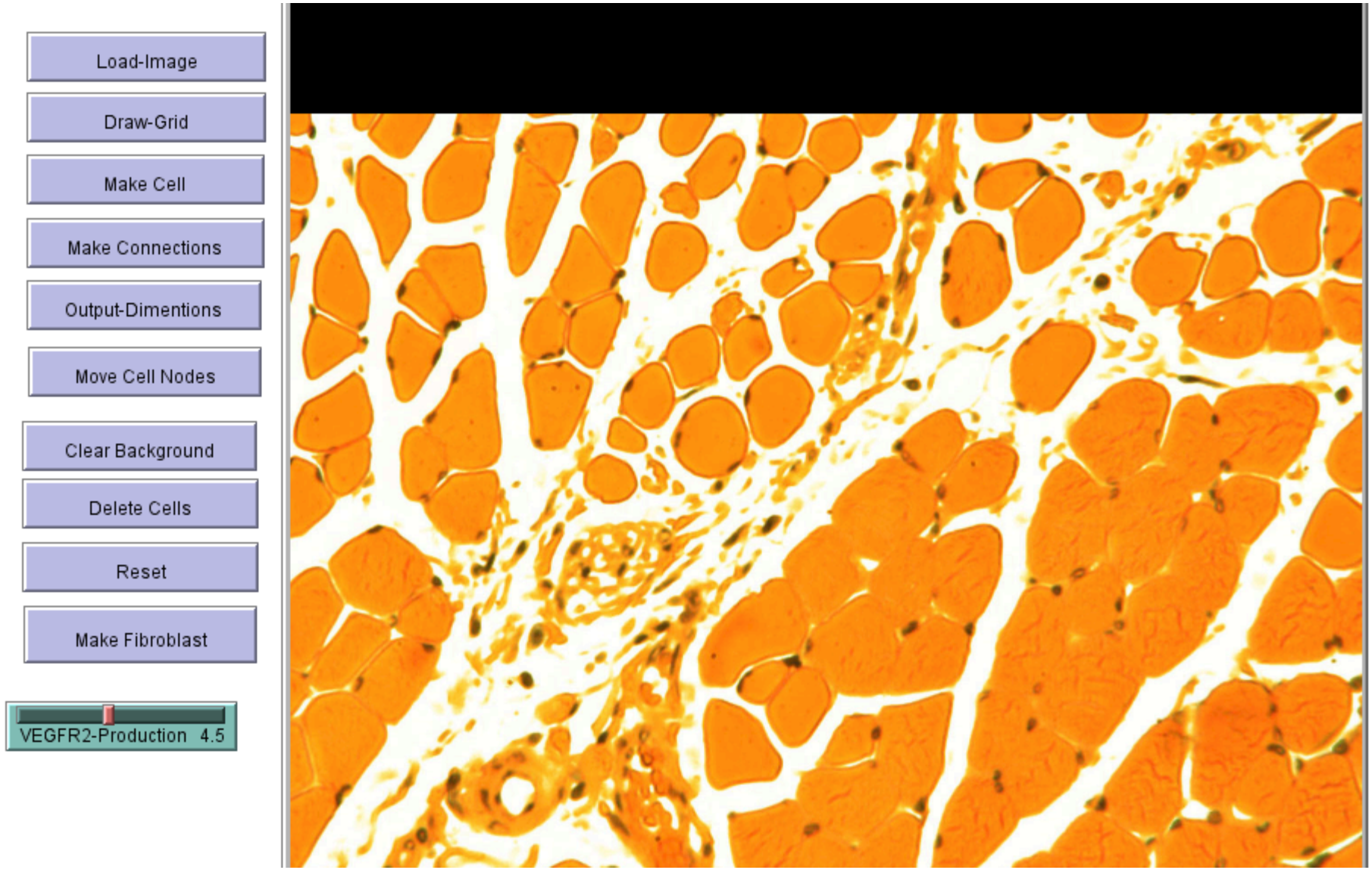

K. Martin, S.M. Peirce, S. Blemker

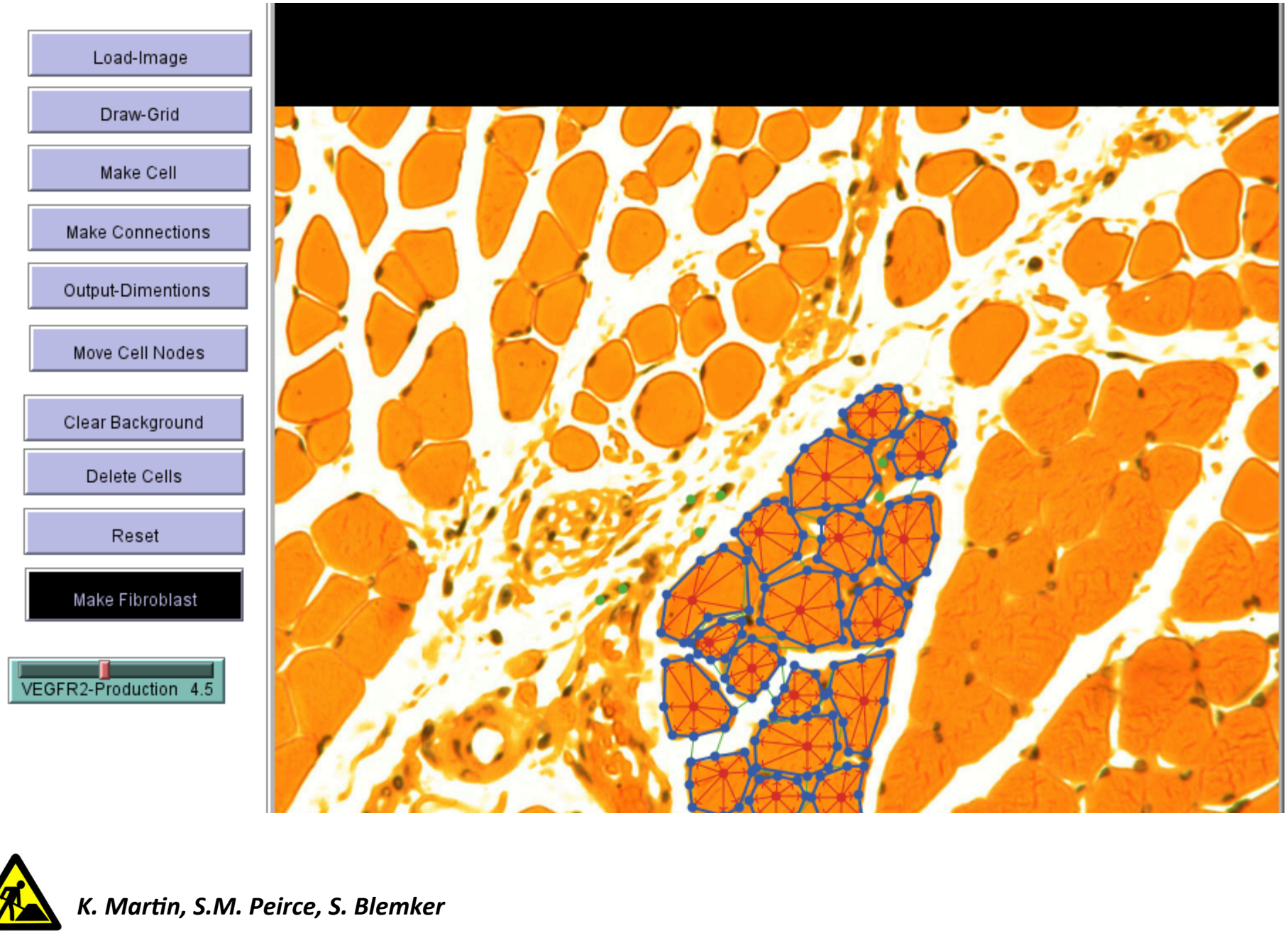

K. Martin, S.M. Peirce, S. Blemker

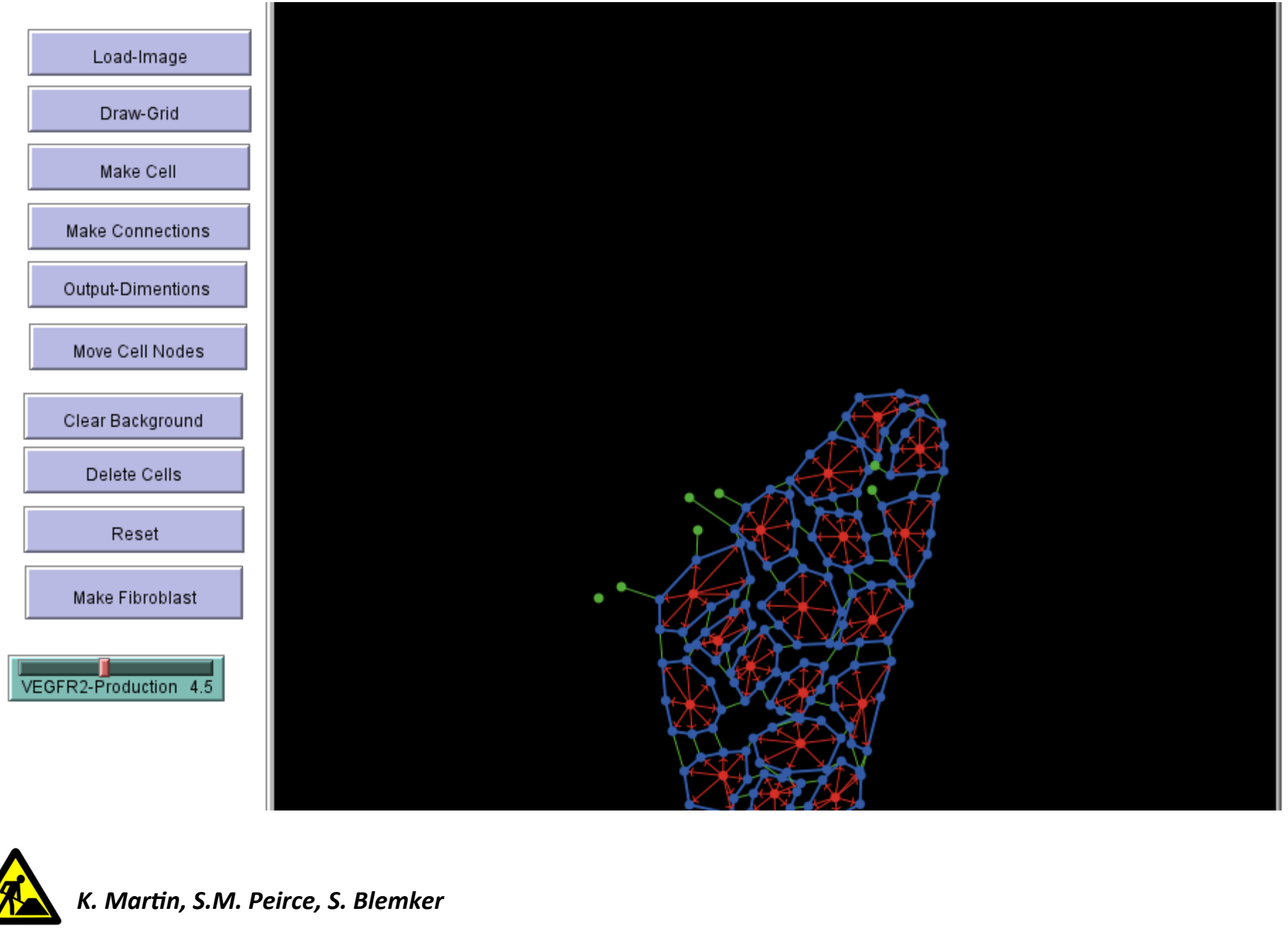

K. Martin, S.M. Peirce, S. Blemker

ACKNOWLEDGEMENTS

Peirce-Cottler Lab

Alex Bailey, Ph.D.
Bryan Thorne, Ph.D.
Alyssa Taylor, Ph.D.
Peter Amos, Ph.D.
Jason Glaw, Ph.D.
Joseph Walpole
Anthony Bruce
Kyle Martin
Scott Seaman
Stephen Cronk

Blemker Lab

Silvia Blemker, Ph.D.
Geoff Hansfield

Papin Lab

Jason Papin, Ph.D.
Erwin Gianchandi, Ph.D.

DeSimone Lab

Doug DeSimone, Ph.D.

Yale University

Jay Humphrey, Ph.D.
Heather Hayenga, Ph.D. (UMD)

UNC-CH

Vicki Bautch, Ph.D.
John Chappell, Ph.D.

Johns Hopkins

Feilim Mac Gabhann, Ph.D.

National Heart Lung and Blood Institute
National Eye Institute
NATIONAL INSTITUTES OF HEALTH
NIAMS
National Institute of Arthritis and Musculoskeletal and Skin Diseases
WALLACE H. COULTER Foundation